# Analysis of the energetic, economic, and environmental performance of hydrogen utilization for port logistic activities

Andrea Mio [a,d], Elena Barbera [b,f,*], Alessandro Massi Pavan [a,d], Romeo Danielis [c,d], Alberto Bertucco [b,e], Maurizio Fermeglia [a,d]

[a] Department of Engineering and Architecture, University of Trieste, Italy
[b] Department of Industrial Engineering (DII), University of Padova, Italy
[c] Department of Economics, University of Trieste, Italy
[d] Center for Energy, Environment and Transport Giacomo Ciamician, University of Trieste, Italy
[e] Centro Studi "Levi Cases" for Energy Economics and Technology, University of Padova, Italy
[f] Department of Civil, Environmental and Architectural Engineering, University of Padova, Italy

## GRAPHICAL ABSTRACT

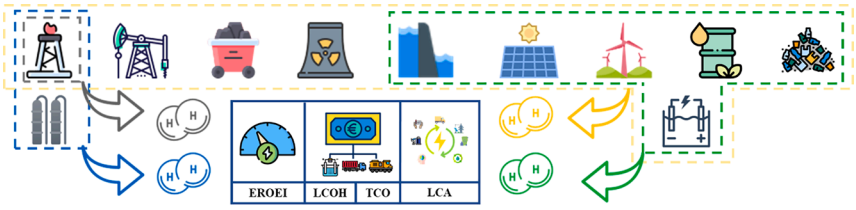


## ABSTRACT

Hydrogen is a versatile energy carrier and storage medium that may be employed in a variety of applications. According to the industrial processes used for its production, hydrogen may be labelled using different colours: (i) grey hydrogen, produced from natural gas using steam methane reforming (SMR), (ii) blue hydrogen, like the grey one, but with carbon capture and storage (CCS), (iii) green hydrogen, produced by water electrolysis using electricity from renewable sources only, (iv) "grid" hydrogen, produced by electrolysis using grid electricity. In this study, process simulation is used to solve material and energy balances, as well as to estimate capital and maintenance costs for each technology investigated. Then, process simulation outcomes are used to estimate three key performance indicators focusing on sustainability issues: the Energy Return on Energy Invested (EROEI), the Levelized Cost of Hydrogen (LCOH) and the Life Cycle Assessment (LCA). With reference to the case study of the Trieste port in Italy, the potential of synthesizing and utilizing hydrogen to fuel transportation activities within a port is examined. Based on the daily hydrogen consumption in fuel cells installed on locomotors and trucks, the design of the different processes considered is carried out, as well as their comparison in terms of EROEI, LCOH, and LCA. Furthermore, LCA and Total Cost of Ownership (TCO) evaluations for various hydrogen-fueled vehicles within the port are presented and compared to diesel-fueled ones to determine the

* Corresponding author at: Department of Industrial Engineering, University of Padova, Via Marzolo 9, 35131 Padova, Italy.
*E-mail address:* elena.barbera@unipd.it (E. Barbera).

impact of fuel-cell vehicles during operations. Results show that EROEI of hydrogen produced by electrolysis is larger than that produced by SMR with or without CCS. The LCOH for grey hydrogen is of the same order of magnitude of that of green or grid ones. The hydrogen compression step to 300 bar impacts on both energetic and economic performances. LCA indicates that the Global Warming Potential (GWP) of green hydrogen is at least half with respect to blue hydrogen, however other impact categories are less favourable. On the other hand, the TCO of hydrogen-fueled vehicles is higher than that of diesel-fueled ones, mainly because of the higher purchase costs. It is concluded that the methodology proposed in this paper, based on the evaluation of indicators at the design stage, is suitable for comparing hydrogen production processes. In addition, it is a powerful tool for policy decision-makers in defining the strategies for the development of hydrogen-based transport systems in port operations.

**Nomenclature**

*Abbreviations*

| | |
|---|---|
| AEA | Aspen Energy Analyzer |
| AEC | Alkaline Electrolysis Cells |
| APEA | Aspen Plus Economic Analyzer |
| BoP | Balance of Plant |
| CAPEX | Capital expenditures |
| CCS | Carbon Capture and Storage |
| CF | Capacity Factor |
| CSRE | Cost for Stack Replacement |
| DGA | Diglycolamine |
| EC | Energy Cost |
| EF | Environmental Footprint |
| Elec-NRTL | Electrolyte Non-Random Two-Liquid |
| EOFP | Photochemical Oxidant Formation including human Ecosystem quality contributions |
| EROEI | Energy Return On Energy Invested |
| FC | Fuel Costs |
| FCI | Fixed Capital Investment |
| FEP | Freshwater Eutrophication Potential |
| FETP | Freshwater Ecotoxicity Potential |
| FFP | Fossil Resource Scarcity |
| FG | Flue Gases |
| GHG | Greenhouse Gas |
| GWP | Global Warming Potential |
| HHV | Higher Heating Value |
| HOFP | Photochemical Oxidant Formation including human Health contributions |
| HP | Hydrogen Production |
| HTPc | Human Toxicity Potential with cancer |
| HTP-nc | Human Toxicity Potential with no cancer |
| IEA | International Energy Agency |
| IPCC | Intergovernmental Panel on Climate Change |
| IRP | Ionizing Radiation |
| LCA | Life Cycle Assessment |
| LCI | Life Cycle Inventory |
| LCIA | Life Cycle Impact Assessment |
| LCOH | Levelized Cost of Hydrogen |
| LOP | Land use Potential |
| MC | Maintenance Costs |
| MEP | Marine Eutrophication Potential |
| METP | Marine Ecotoxicity Potential |
| NEA | Net Energy Analysis |
| NG | Natural Gas |
| NRTL | Non-Random Two-Liquid |
| ODP | Stratospheric Ozone Depletion |
| OPEX | Operating expenditures |
| PEMEC | Proton Exchange Membrane Electrolysis Cells |
| PMFP | Fine Particulate Matter Formation |
| PR-BM | Peng-Robinson equation of state with Boston-Mathias modifications |
| PS | Process Simulation |
| PSA | Pressure Swing Adsorption |
| PV | Photovoltaics |
| RD | Refueling Dispenser |
| RKS-BM | Redlich-Kwong-Soave equation of state with Boston Mathias modifications |
| SC | Start-up Cost |
| SGTC | Sequential Gas Turbine Combustion |
| SMR | Steam Methane Reforming |
| SOEC | Solid Oxide Electrolysis Cells |
| SOP | Mineral Resource Scarcity |
| TAP | Terrestrial Acidification Potential |
| TCO | Total Cost of Ownership |
| TEN-T | Trans European Network Transport |
| TETP | Terrestrial Ecotoxicity Potential |
| TIC | Total Installed Cost |
| TRACI | Tool for Reduction and Assessment of Chemicals and Other Environmental Impacts |
| TRL | Technology Readiness Level |
| WCP | Water Consumption Potential |
| WE | Water Electrolysis |
| WGS | Water-Gas Shift |
| WTW | Well-to-Wheel |

*Parameters*

| | |
|---|---|
| $EL_{cost}$ | cost of electricity |
| $L_{el}$ | electrolyser lifetime |
| $NG_{cost}$ | cost of natural gas |
| $P_{aux}$ | power energy supplied to process auxiliaries |
| $P_{elec}$ | Power energy supplied to electrolysers |
| $Q_{H2}$ | hydrogen outlet flow rate |
| $Q_{NG}$ | natural gas inlet flow rate |
| $V_{act}$ | activation overpotential |
| $V_{cell}$ | cell voltage |
| $V_{conc}$ | concentration overpotential |
| $V_{ohm}$ | ohmic overpotential |
| $V_{rev}$ | reversible voltage |
| $s_{o\&m}$ | share of the investment costs dedicated to operation and maintenance |
| $\varepsilon_c$ | proportionality coefficient between costs of energy and capital costs |
| $L$ | plant lifetime |
| $cf$ | capacity factor |
| $r$ | discount rate |
| $\eta$ | efficiency of transformation for the process of interest |

*Subscripts*

| | |
|---|---|
| *Aux* | auxiliaries |
| *Cap* | capital |
| *f* | fuels |
| *H2* | hydrogen |
| *in* | inlet |
| *o&m* | operation and maintenance |
| *out* | outlet |
| *t* | value at year t |

## 1. Introduction

Energy needs have increased rapidly over the last few decades, putting growing strain on the energy industry. Primary energy consumption rate varies by country and location, with the global average rising dramatically from 2000 to 2020 by roughly 53%, from 377 EJ/year in 2000 to 579 EJ/year in 2020 [1]. Recent reports of IPCC [2] and IEA [3] indicate that a strong reduction in the use of fossil fuels must be achieved in order to meet the 2030 greenhouse gases emission targets. Thanks to its ability to compensate fluctuation in the renewables, hydrogen ($H_2$) is a suitable energy carrier for several applications in heavy transportation, logistic and energy-hard-to-abate sectors [4].

In line with the European Hydrogen Strategy [5], numerous member nations in Europe, including France, Germany, and Spain, have already developed ambitious plans for this energy carrier. The Italian National Recovery and Resilience Plan [6] has allocated 3.2 billion euros for research on $H_2$, which should help Italy in its decarbonization path. It is envisaged that $H_2$ may soon be able to power trains, trucks and ships. Undoubtedly, it could stabilize the electrical grid and decarbonize heavy industry operations. However, in order to do so, its production needs to be significantly increased, which can only be deemed clean and sustainable if it emits no Green House Gases (GHG). At present, 95% of the $H_2$ produced in the world comes from steam methane reforming (SMR) and only 5% using direct water splitting through electrolysis [7].

Experts currently agree on assigning $H_2$ a niche role, useful for decarbonizing "hard-to-abate" sectors, and on leaving the predominant role in the transition to direct electrification [8]. Consequently, it is necessary to carefully evaluate the $H_2$ production processes for those sectors where it is essential. To do so, it is important to base decisions on careful process design and clear and universally accepted indicators.

A number of indicators are available in the literature and should be employed by decision-makers. One of them is the Energy Return on Energy Invested (EROEI) [9], that relates the amount of net energy stored in the $H_2$ produced to the total energy invested in the process. EROEI has recently been proposed as a benchmark tool by the International Energy Agency (IEA) in the guideline methodology for the net energy analysis [10].

Another key performance indicator, specific for $H_2$, is the Levelized Cost of Hydrogen (LCOH), which considers the cost of the $H_2$ production process and is calculated as the ratio between the net discounted costs over the amount of $H_2$ produced [11]. Inputs to LCOH include capital and investment costs, operation and maintenance costs on yearly basis, and plant lifetime.

These two indicators focus on $H_2$ production processes in terms of energy consumption and economic analysis, but are insufficient for evaluating their overall environmental impacts. Indeed, Life Cycle Assessment (LCA) [12] is a suitable tool to provide a complete panorama of the environmental burdens generated by processes and products [13–15].

Finally, the Total Cost of Ownership (TCO), which is the cost of purchasing something plus the cost of operating it during its useful life, is an indicator widely employed in the economic evaluation of transportation. The TCO, if coupled with EROEI, LCOH, and LCA, assists decision-makers in making informed choices.

Ports are large contributors to $CO_2$ and local air pollution emissions. Cigolotti [16] argued that the 1400 European ports generate about 4.7% of the total $CO_2$ emissions in Europe. Air emissions derive both from port operations and from vessels, trains and trucks arriving or leaving the port. Additionally, it should be noted that the environmental impacts from ports frequently occur adjacent to metropolitan areas, making the need to lead ports towards a more sustainable set up even more compelling. The "green port" concept encompasses a set of strategies to improve energy efficiency and reduce local and global air pollution. Therefore, the management of port operations may be of great interest. Energy duties of port operations are mainly due to people and cargo handlings, and are currently met by fossil fuels. Alternatively, they could be powered by both electricity and hydrogen. It is known that, in transportation, fuel cells applied to $H_2$ vehicles can provide more power density than batteries, and therefore seem suitable for heavy loads [17]. In addition, fuel cells with the same footprint compared to traditional lithium-ion batteries allow an autonomy about three times greater and could therefore help decarbonizing the heavy transport.

Shipping is a hard-to-abate sector, due to the high energy intensity required, which cannot be supplied by batteries. Here, not only $H_2$, but also ammonia and methanol are the solutions currently being explored [18]. According to a recent report by IRENA [19], in 2050 the naval sector is expected to require 46 million tons of green $H_2$, the majority of which (73%) will be used to produce ammonia, covering almost half of naval energy consumption. However, 183 million tons would be needed, equivalent to today's world production of ammonia for all uses.

Despite being the most electrified mode of transportation, trains are still powered by diesel on some routes where access to electricity is still problematic. In Italy, 28% of the railways run with diesel locomotors and it could make sense to convert them to $H_2$: it is no coincidence that the preliminary guidelines of the National Hydrogen Strategy have among their 2030 objectives the conversion to hydrogen of 50% of the non-electrified routes [20]. Within port gates, trains are often assembled using diesel locomotors, which indeed could be substituted with fuel-cells powered ones.

Port areas represent a good opportunity for *in loco* hydrogen production, avoiding the issues associated with its transport and storage. Hydrogen may be produced using different industrial processes, each one identified by a colour. Besides grey $H_2$, which is obtained by natural gas steam reforming and emits to the atmosphere 9–11 $kgCO_2/kgH_2$ plus all the emissions related to natural gas procurement, three other processes appear more environmentally friendly and will be considered in this work: (i) green $H_2$, produced by electrolysis of water using electricity from renewable sources, (ii) grid $H_2$, obtained by water electrolysis using grid electricity, (iii) blue $H_2$, which is like grey $H_2$, but with carbon capture and storage (CCS).

Many papers have been published in the last few years, assessing the performances of one or more hydrogen production pathways, and comparing them from either energetic, economic, or environmental standpoints [21]. In a purely economic perspective, the analysis of the literature suggests that $H_2$ production from fossil fuels currently represents the most convenient pathway. Lee et al. report a LCOH from SMR of 1.8–2.3 $\$/kgH_2$ [22], while Ali Khan et al. identify a range between 1.38 and 2.3 $\$/kgH_2$ for grey hydrogen, which increases to 2.0–3.42 $\$/kgH_2$ with the addition of CCS for blue hydrogen, depending on the price of natural gas [23]. Fan et al., instead, compare the LCOH of hydrogen production from coal (with and without CCS) with that of water electrolysis, concluding that the latter is 20%-60% higher than the former [24]. On the other hand, when considering environmental impacts, it is not clear yet which pathway could be more sustainable [7,25,26]. Bauer and co-authors made a detailed comparison between GHG emissions of grey, blue, green and grid hydrogen [25]. A thorough life-cycle greenhouse gas emissions and net energy analysis of photovoltaics-powered water electrolysis was carried out by Palmer and co-authors, highlighting EROEI values between 3 and 7, depending on the conditions, and GHG strongly dependent on grid buffering imports [27]. Zhao et al. quantitatively compared the environmental performances of different water electrolysis technologies, focusing mainly on the impacts due to the consumption of critical materials needed for the construction of electrolytic cells [28].

To the best of the authors' knowledge, no studies compare the different hydrogen production technologies considering all the indicators reported above, i.e. EROEI, LCOH, LCA, and TCO. Only very few studies are present in literature simultaneously considering EROEI, LCA and LCOH evaluation [29,30], but none of them consider the TCO and, above all, they are not based on process simulation for the estimation of the necessary parameters. Most of the available papers focused on single aspects, without adopting an interdisciplinary approach. Additionally,

rather than referring to a specific and practical situation, the comparison of various hydrogen colours is frequently approached from a generalized and absolute standpoint, leading to findings that can be problematic depending on the underlying assumptions [7,25,26]. For these reasons, the aim of the present work is to analyse and assess the sustainability of on-site hydrogen production and its use to power port operations, comparing different technologies. Detailed Process Simulations (PS) will be applied to allow the evaluation of EROEI, LCOH, LCA and TCO on a rigorous and systematic approach.

As a real-world example of a medium-sized Mediterranean port that is rapidly expanding and where the port authority is seriously contemplating investing in hydrogen for its logistic, the port of Trieste, located in the North East of Italy, will be used as the case study. Being surrounded by the city of Trieste, its environmental footprint is part of the political debate. Its geographical position at the intersection between shipping routes and the Baltic-Adriatic and Mediterranean TEN-T core network corridors, makes it an international hub for Central and Eastern Europe. Trieste is the final destination of direct ocean transportation services of the world's main shipping lines to China, the Far East, Singapore and Malaysia, with stops in several other ports in the Mediterranean Sea. Rail development as a preferred option for hinterland connections has been a key component of the port strategy over time. More than 400 trains a month link Trieste to the manufacturing and industrial areas of North-East Italy and Central and Easter Europe. Two specialized companies, Alpe Adria S.p.A. and Adriafer, organize train services and operate the trains inside the port, respectively. A 70 km internal rail network allows all docks to be served by rail with the possibility of shunting and/or assembling freight trains directly in the various terminals. So far, all shunting trains are diesel-fueled. This paper evaluates the possibility of replacing diesel-fueled locotractors with $H_2$-fueled ones. In addition, it considers the use of $H_2$ yard trucks for cargo-handling in container terminals, that represents the single largest source of emissions in all classifications of cargo handling equipment [31]. This is particularly relevant in relation with the small size of the hydrogen production processes considered, which is typical of a locally intended use, and significantly smaller compared to the production rates required, for example, by a refinery. A special feature of our case study is that $H_2$ is produced and consumed within the port boundaries, so there is no energy duties and monetary costs associated with $H_2$ transportation. As a result, the study outlines the optimum technological and financial circumstances for the replacement of diesel with hydrogen as the primary energy source of medium-size port areas. Despite this paper focuses on the special case of the port of Trieste, the proposed methodology is general and could be applied to any port, or logistic centre, in which trucks, trains and other means of transportation are in operation.

In summary, it is proposed to use PS to obtain all the data needed to evaluate the desired indicators, with material and energy balances calculated using reliable and validated models. PS is a mature tool that solves material and energy balances for chemical [32] and biochemical [33] processes, and is reliably used for process design, optimization, and feasibility studies. Moreover, PS can provide an energetic and an economic evaluation of the process. Performance indicators for all desired metrics and impact categories can be obtained by combining PS with EROEI estimation, LCOH calculation, TCO evaluation, and the LCA approach. By applying a comprehensive process simulation-based study, the sustainability of the proposed technical solution may be assessed at an early stage [34], giving decision-makers a powerful tool that is already available at design time. In the open literature, PS has been systematically coupled with LCA in a number of studies [35–38], according to the methodology proposed by Morales-Mendoza et al. [39]. On the other hand, a very limited number of papers used PS to evaluate the EROEI of chemical processes [33,40–42], and for LCOH calculation [43], but without applying a systematic approach, and apparently no work has been extended to include TCO evaluation to PS.

The novelty of this paper is threefold: firstly, different electrolyser technologies are comprehensively simulated and optimized, as well as two CCS configurations integrated with SMR, specifically tailored to the characteristics of the inlet gaseous stream. Secondly, process simulation results in terms of mass balance, energy balance and equipment cost evaluation have been used for the *a priori* estimation of relevant indicators such as the EROEI, LCOH, TCO and LCA, which has never been applied before. Thirdly, to the best of authors' knowledge, a thorough analysis of the energy, environmental and economic features at port level is not available in the literature. Thus, these indicators are valuable to define long-term strategies for the development of national and international energy systems based on $H_2$ in port operations.

The paper is organized as follows: section 2 presents the methods applied, including the details about process simulation, the calculation of the EROEI, LCOH, TCO and LCA; section 3 provides and discusses the results obtained with the methods previously described; lastly, some final remarks are reported in section 4.

## 2. Methods

All process simulations were carried out using Aspen Plus v. 12.1. The software allowed to develop the process flowsheet for each hydrogen production process considered, and to perform physical property estimations, material and energy balances, design/rating calculations, sensitivity analysis and process optimization. In addition, heat integration by pinch analysis was performed with Aspen Energy Analyzer (AEA) to minimize the energy duties, while economic evaluation to retrieve the capital and operating costs of each process was performed with Aspen Process Economics Analyzer (APEA).

### 2.1. Hydrogen production for Trieste port

The analysis is carried out with reference to a daily hydrogen production corresponding to the estimated hydrogen consumption required by the considered logistic activities in the port of Trieste. These are the use of hydrogen in fuel cells-equipped train locomotors and trucks, operating on rails and roads in the port of Trieste. The hydrogen production processes considered in the work are sized according to the daily requirement, reducing the need to store high amounts of hydrogen within the port. A storage tank of hydrogen gas has been included in the system to guarantee the storage needed to sustain one production day.

According to the mobility data of diesel train locomotors within the port measured during the first 3 months of 2022, the average diesel consumption per locomotor is 12.1 l/h, (i.e., 10.11 kg/h). Given that locomotors are not moving continuously throughout the day, a daily average use of 18 h per day results in 182 kg of diesel daily consumption. Considering 5 locomotors, the total daily consumption of diesel oil is estimated to be 910 kg/day [44]. Concerning trucks, the average consumption of diesel oil is around 40.6 l (i.e., 33.9 kg) for 100 km. Considering 15 trucks running for 300 km every day, the total daily consumption of diesel oil for trucks is 1525.5 kg/day. Summing up the two contributions, a total diesel oil consumption of 2435.4 kg/day is calculated.

Considering that one unit of hydrogen mass has as an energy content about 3.1 times that of diesel oil, the daily amount of hydrogen to be supplied to locomotors and trucks is about 800 kg/day. This is considered to be produced locally. The different production processes compared for this purpose are described in the following sections. In all the cases considered, compression of the product up to 300 bar was set, to comply with utilization in fuel cell vehicles. A buffer storage of gaseous hydrogen at 300 bar made up of 12 storage tanks with a capacity of 3300 l each, (able to store 70.8 kg of hydrogen at 300 bar) was included in the design as well as the fuelling station for hydrogen users.

A schematic of the system is represented in Fig. 1.

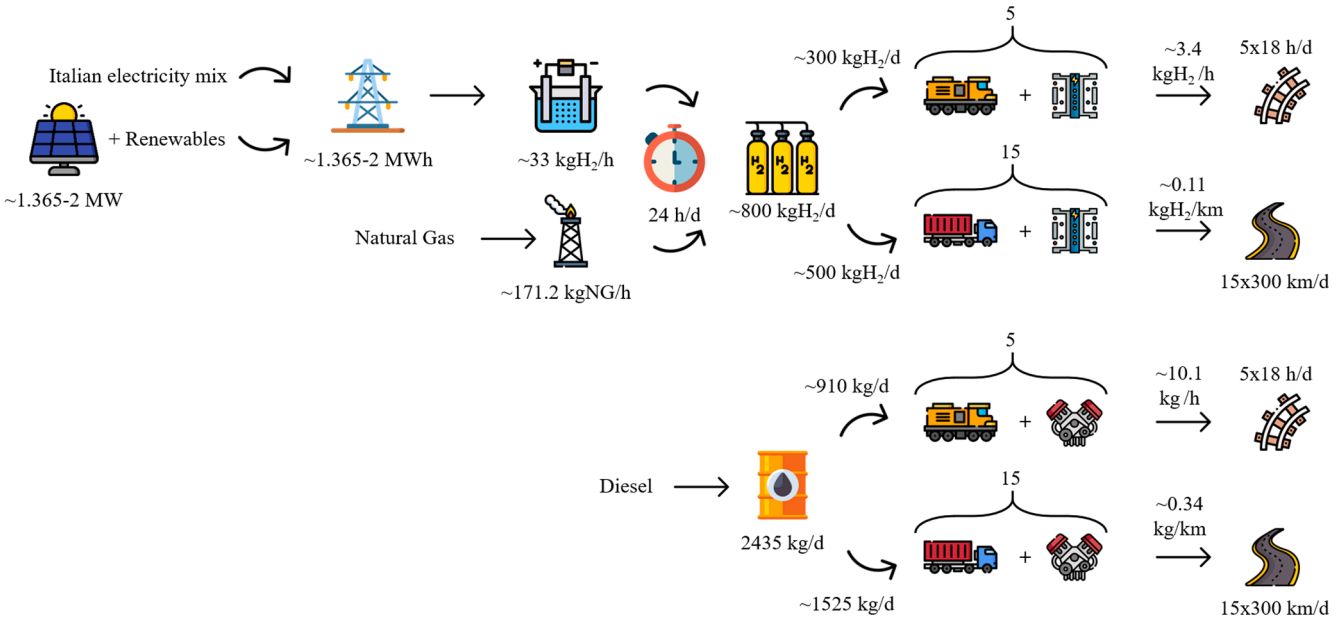


**Fig. 1.** Electricity and fuel demands for supporting the logistics activities of the port.

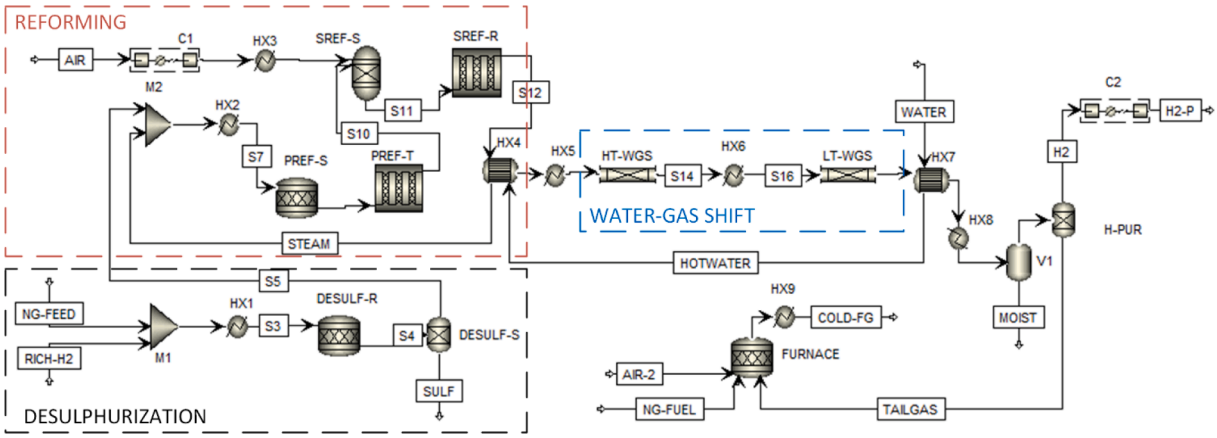


**Fig. 2.** Aspen Plus process flowsheet of the SMR process. Tags on streams and blocks identify the main streams and unit operations, whose features are summarized in Table S1 and S2, respectively.

### *2.2. Grey hydrogen: steam methane reforming production process*

Grey hydrogen is obtained from natural gas via steam methane reforming (SMR). The SMR process flowsheet was adapted from the corresponding section of the ammonia production process simulation available in the Aspen Plus database [45], properly downscaled to meet the daily hydrogen production of 800 kg/day. The Redlich-Kwong-Soave equation of state with Boston Mathias modifications (RKS-BM) was used as thermodynamic model in all of the process units. The process flow diagram is shown in Fig. 2.

The process is divided into a number of sections. The natural gas (NG) feed first undergoes a desulphurization treatment to remove sulphur, which is reduced to hydrogen sulphide by catalytic hydrogenation, and $H_2S$ is then removed by adsorption with zinc oxides. The reforming unit comprises a primary reformer (PREF-T), where the desulphurized feed is converted to $H_2$ and carbon oxides in the presence of steam, and a secondary reformer (SREF-R), where compressed hot air is added. The main reactions occurring in the reformers involve the catalytic conversion of methane into a mixture of CO, $CO_2$ and $H_2$, at high temperature and pressure (T = 500–1200 °C, P = 30–34 bar) over Ni catalyst supported on alumina ceramics. The reformers are modelled as plug-flow reactors (RPlug), where reaction kinetics, heat transfer rate (the net reaction is endothermic), and pressure drops are rigorously modelled by means of Fortran user subroutines [45].

To increase the hydrogen yield, the CO contained in the reforming products is catalytically converted to $CO_2$ and $H_2$ according to the exothermic water–gas shift (WGS) reaction in two stages: the first at high temperature (HT-WGS, T = 380–460 °C, P = 30 bar), over iron oxide catalyst, and the second one at lower temperature (LT-WGS, T = 210–270 °C, P = 28 bar), over copper oxide catalyst. The units are modelled as adiabatic plug-flow reactors (RPlug), and the reaction kinetics has been implemented in a Fortran user kinetics subroutine.

Following WGS conversion, the product gases are cooled down to a temperature of 40 °C. After moisture removal in the flash vessel V1, hydrogen is purified by means of pressure swing adsorption (PSA), modelled as a simple Sep unit in Aspen (H-PUR). Pure hydrogen is recovered at a pressure of 26.7 bar, and then compressed to a final pressure of 300 bar by 2-stage compression (C2, pressure ratio = 3.35) with intercooling at 45 °C and final cooling to 25 °C. The tail gases stream, containing unreacted $CH_4$ and CO, as well as the produced $CO_2$ (45 mol%) and $N_2$, is recovered at a pressure of 1.5 bar, and delivered, together with additional natural gas (NG-FUEL), to the furnace, to

supply the heat necessary for the endothermic reforming reaction. The furnace is modelled as a stoichiometric reactor (Rstoich) where combustion reactions occur. The heat duty is set so to match that required in the primary reformer. The flue gases produced by the combustion are cooled from 780 °C to 355 °C.

Given the small scale of the production plant, the main process equipment (i.e., reformers and WGS reactors) were designed considering small modular systems, as described in the report by the National Renewable Energy Laboratory (NREL) [46] which refers to a daily $H_2$ production of 110 kg/d, and their cost calculated accordingly. Details on the main process units as well as complete stream tables are provided in the Supplementary Material.

### 2.3. Blue Hydrogen: steam methane reforming with CCS

Blue hydrogen indicates $H_2$ produced via SMR, coupled with a Carbon Capture and Storage (CCS) system to lower the $CO_2$ emissions directly related to the former process. Specifically, SMR generates two $CO_2$ emissions: process emissions, i.e., those related to the actual SMR and WGS reactions, and combustion emissions, i.e., those generated by the combustion of natural gas and of the tail gases recovered after $H_2$ purification in the furnace. Accordingly, CCS could be applied either on the tail gases stream (thus capturing only process emissions) or on the flue gases stream, which includes both process and combustion emissions. These two streams differ significantly in terms of $CO_2$ partial pressure and flow rate: tail gases are characterized by a high $CO_2$ concentration, which makes its capture more favourable and less energy-intensive compared to more diluted flue gases. However, a significant amount of $CO_2$ would not be captured [47]. For completeness, both options have been considered in this analysis, and two different CCS process simulations were developed, coupled with the tail gases and flue gases obtained by the simulation of SMR, respectively. Only the process flowsheet corresponding to the first option (tail gases CCS) is reported (Fig. 3). The configuration regarding flue gases CCS is similar, with only minor differences (Figure S1 of Supplementary Material).

Carbon capture is achieved by means of chemical scrubbing with amines. Specifically, an aqueous solution with about 37 wt% diglycolamine (DGA) is used as capturing solvent (LEANIN), and is fed at 55 °C at the top of the absorber counter-current to the tail gases (or flue gases) stream, at 40 °C. To avoid excessive amine losses due to entrainment with the clean gases exiting from the top (GASOUT), a washing section is present at the top of the absorber, where water is recirculated to capture the volatile DGA. The absorption unit is designed to capture 85–90% of the $CO_2$ from the inlet stream. The clean gases stream is then cooled down to 40 °C, to separate the condensate in V1, as they are then sent to the SMR furnace with natural gas to supply the heat required by the reformer. The drying step is not present in the flue gases CCS configuration, where the clean gases are vented to the atmosphere.

The rich solution from the bottom of the absorber (RICHOUT), after heat recovery in the heat exchanger HX1, is sent to the regeneration unit at a temperature of 106 °C (RICHIN). Solvent regeneration occurs by means of reboiled stripping. The gaseous stream recovered from the top of the stripper at nearly 105 °C is cooled down to 15 °C, and the liquid fraction (REFLUX) is recycled to the top of the column, while the purified $CO_2$ is compressed from atmospheric pressure to 150 bar for the subsequent transport and sequestration [15]. The regenerated solution (LEANOUT), at 127 °C, exchanges heat with the rich solution in HX1, and is recycled back to the absorber, after solvent make-up.

The absorption and stripping columns were modelled according to a rigorous rate-based procedure, considering packed columns filled with 700Y FLEXIPAC® Structured Packing by Koch. The thermodynamic model used in the simulation was the Electrolyte Non-Random Two-Liquid (Elec-NRTL), except for the $CO_2$ compression unit, where the Peng-Robinson equation of state with Boston-Mathias modifications (PR-BM) was selected. More details on the main process units as well as complete stream tables for both tail gases and flue gases CCS are provided in the Supplementary Material.

### 2.4. Green Hydrogen: water electrolysis from renewables

Green hydrogen identifies $H_2$ obtained from the electrolysis of water powered by renewable energy sources, including photovoltaics, wind, hydro, geothermal, biomass and urban waste incineration.

For green hydrogen, it is assumed that the electrolysers operate at a high capacity factor (cf = 0.97), using all the electrical energy supplied by a local photovoltaic (PV) system with a total installed capacity

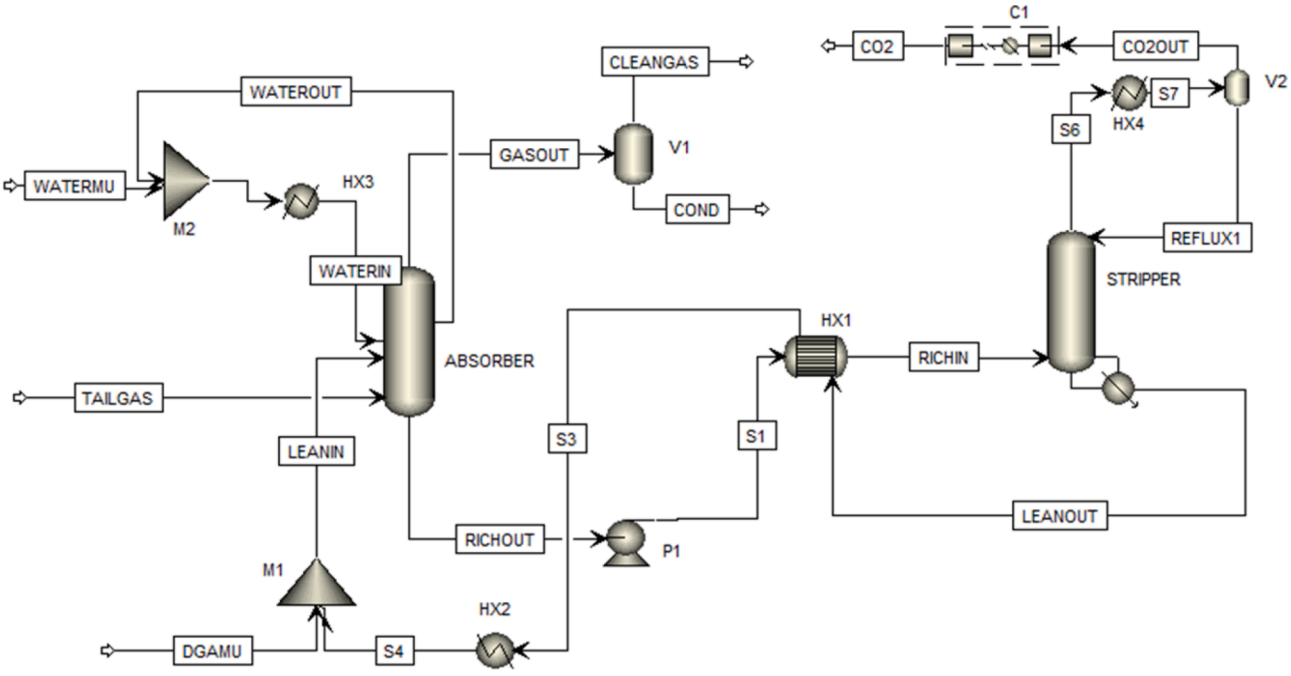


**Fig. 3.** Aspen Plus process flowsheet of CCS performed on the tail gases from SMR. Tags on streams and blocks identify the main streams and unit operations, whose features are summarized in Table S3 and S4, respectively.

equivalent to the peak electrolyser's need, and the remaining energy requirement supplied by an Italian green grid energy provider. Accordingly, the installation cost of the PV plant, as well as the cost of green energy from the provider, are taken into account in the evaluation of the indicators (section 2.6).

Water electrolysis (WE) is the electrochemical splitting of water into hydrogen and oxygen, thanks to the application of an electrical voltage. The voltage that needs to be applied to the electrolytic cell ($V_{cell}$) is given by the sum of the reversible voltage $V_{rev}$ (i.e., the minimum voltage required for the reaction to occur, determined by thermodynamics) and a series of overvoltages caused by ohmic resistances ($V_{ohm}$), limitations in electrode kinetics (i.e., activation overvoltage, $V_{act}$), and mass transfer (i.e., concentration overvoltage $V_{conc}$). Water electrolysis technologies are classified according to the type of electrolyte used to separate the two half-reactions occurring at the anode (oxygen evolution reaction) and at the cathode (hydrogen evolution reaction). Currently, three technologies are being considered for green hydrogen production, namely Alkaline Electrolysis Cells (AEC), Proton Exchange Membrane Electrolysis Cells (PEMEC), and Solid Oxide Electrolysis Cells (SOEC). The first two have already reached technological maturity, while the latter is still at the development stage. However, all of these three technologies are considered in the analysis, and have been simulated in Aspen Plus. Electrolysis processes comprise the cell stack (i.e., a number of electrolytic cells connected in series), which is the heart of the process, as well as the balance of plant (BoP), which includes all the other units necessary for product purification, liquid recirculation, and so on. In the next sections, the three electrolysis processes and the corresponding Aspen Plus models (Fig. 4) are briefly described. Since electrolysis stack models are not implemented in Aspen Plus, the corresponding material and energy balance equations were inserted by means of a user defined unit block coupled with Microsoft Excel.

#### 2.4.1. Alkaline electrolysis cell (AEC)

The AEC process flowsheet developed in Aspen Plus is shown in Fig. 4A. In the stack, the electrodes are immersed in a liquid electrolyte separated by a diaphragm. The electrolyte solution (STACK-IN, with 35 wt% KOH) is continuously recirculated within the stack. Water is consumed at the cathode side and produced at the anode side, so that the two liquid streams have to be mixed before entering the electrolyser. Material and energy balances were calculated according to the model proposed by Sánchez et al. [48], which includes the calculation of cell voltage, Faraday efficiency, and gas product purity as a function of temperature, pressure, and current density. From these, it is possible to calculate the stack power ($W_{stack}$), as well as the hydrogen and oxygen production rates, and the heat release ($Q_{stack}$). Based on the results reported by the same authors, operating conditions were set at 80 °C, 5 bar, and 2500 A/m$^2$, using 100 cells connected in series, with an active area of 4.2 m$^2$ each. The detailed model equations are reported in the Supplementary Material.

The product gases generated at the cathode (H2-STACK) and at the anode (O2-STACK) together with the liquid electrolyte are sent to liquid–gas separation vessels (SEP-H2 and SEP-O2, respectively). The recovered liquid electrolyte is then recirculated, with a make-up of deionized water fed to the oxygen separation vessel, while the gases pass through water traps to remove humidity. Finally, $H_2$ is compressed to the final pressure of 300 bar by means of a 4-stage isentropic compression (pressure ratio 2.87), with intercooling at 45 °C and final cooling at 25 °C. The Elec-NRTL model was used for all the process units, except for $H_2$ compression, where the Peng-Robinson equation of state (PR) was employed.

#### 2.4.2. Proton exchange membrane electrolysis cell (PEMEC)

The Aspen Plus flowsheet of a PEMEC electrolyser is shown in Fig. 4B. In this case, a solid polymeric proton exchange membrane made of Nafion® 117 separates the two electrodes, which, due to the corrosive environment generated by the passage of protons, are made of noble metals (Pt for the cathode and Ir for the anode), and water is fed to the anodic compartment. Material and energy balances in the stack were calculated according to the semi-empirical model by Dale et al. [49], which calculates the cell voltage $V_{cell}$ as the sum of the reversible Nernst voltage ($V_{rev}$, function of temperature and pressure according to thermodynamic principles), and temperature/current density-dependent ohmic ($V_{ohm}$) and activation ($V_{act}$) potentials. The hydrogen and oxygen production rates are calculated as in the case of AEC electrolysers, assuming a Faraday efficiency of 100% [50]. A spillover of water occurs across the membrane from the anode to the cathode side, mainly proportional to the proton flow. Specifically, 8 molecules of water are assumed to be dragged per molecule of hydrogen produced [51]. An excess of water circulates in the cathode, in order to remove the heat released by the process: the amount of circulating water is calculated so to allow a temperature increase of 1 °C between inlet and outlet. The detailed equations are provided in the Supplementary Material. The stack is made of 500 cells, with an active area of 0.11 m$^2$ each. Based on the results reported by the authors [49], the stack is operated at 60 °C, 1 bar, and with a current density of 16,000 A/m$^2$. The biphasic water-oxygen (O2-STACK) and water-hydrogen (H2-STACK) streams are sent to liquid–gas separation vessels. The liquid phase recovered from the H2-SEP is fed to the oxygen separator together with the deionized water make-up (H2O-FEED), and the total liquid flow is then fed to the stack. The product gases are cooled down to 25 °C and humidity is removed. $H_2$ is then compressed to the final pressure of 300 bar by means of 4-stage isentropic compression (pressure ratio = 4.16), with intercooling at 45 °C and final cooling at 25 °C. The NRTL activity coefficient model with Redlich-Kwong (RK) equation of state for the gaseous phase was used to model the thermodynamic behaviour, except for $H_2$ compression, where the PR equation of state was used.

#### 2.4.3. Solid oxide electrolysis cell (SOEC)

SOEC electrolysis (Fig. 4C) differs from the previous two because it is operated at high temperature, so that water is fed in the gaseous phase as steam. The solid electrolyte, cathode and anode are made of yttria-stabilized zirconia (YSZ), Ni-YSZ and a mixture of YSZ and Sr-doped La (LSM-YSZ), respectively, and the corresponding thickness are 50, 50, and 500 μm [52]. The stack is composed by 12 modules of 740 cells with an active area of 0.04 m$^2$ each, as larger sizes have not been developed yet. Steam is fed to the cathode side, together with a fraction of recycled hydrogen to maintain reducing conditions (FEED-CAT, $H_2O$: $H_2$ ratio = 10:1), while negatively charged $O^{2-}$ anions diffuse through the electrolyte towards the anode. Air is instead fed at the anode (AIR-HOT) as a sweep stream to remove the produced oxygen. Both the air and water feeds are preheated using the hot products leaving the stack (O2-STACK and H2-STACK). However, due to the difference in heat capacity between inlet steam and outlet products, the feed steam needs to be further superheated by an external source to reach the operating stack temperature. The operating conditions were set at 800 °C, 1 bar, and 2500 A/m$^2$ [52,53]. The steam-hydrogen product mixture is then cooled down to 25 °C and the condensed water is separated. A fraction of the dry product hydrogen is then recycled, while the remaining product is compressed up to 300 bar by means of 4-stage isentropic compression (pressure ratio = 4.16) with intercooling at 45 °C and final cooling to 25 °C. The PR equation of state was used as thermodynamic model in all of the process units. The detailed electrochemical model equations and process stream tables are reported in the Supplementary Material.

The main characteristics and performances of the electrolysers technologies considered are summarized in Table 1.

### 2.5. Grid hydrogen: water electrolysis from grid

The energy mix considered for grid hydrogen is that of Italy in 2020, as reported in Table 2. In the same table, the mix taken from the green electricity provider used for green hydrogen is reported. In this case, the entire amount of electrical energy necessary to obtain the desired

hydrogen production, with the electrolysers working at high capacity factor (cf = 0.97), is taken directly from the grid with the specified energy mix, which includes both renewable and fossil sources.

### 2.6. Capital and operating costs

Capital costs (CAPEX) (€) for all the considered processes are calculated directly from the output of the Aspen Plus Economic Analyser. Specifically, the value of the total installed cost (TIC) from Aspen Plus (which corresponds to the so-called "Inside Battery Limits" or "ISBL" costs in the methodology proposed by Douglas [58]) is used to estimate the Fixed Capital Investment (FCI), and the Start-up Cost (SC) is assumed to be 10% of FCI, according to:

$$CAPEX = FCI + SC = 1.1 \cdot FCI = 1.1 \cdot \frac{TIC}{0.6} \quad (1)$$

For green hydrogen, CAPEX includes the cost of installation and purchase of the PV system.

As far as operating costs (OPEX) are concerned, they are distinguished between fixed and variable ones. For SMR and SMR + CCS

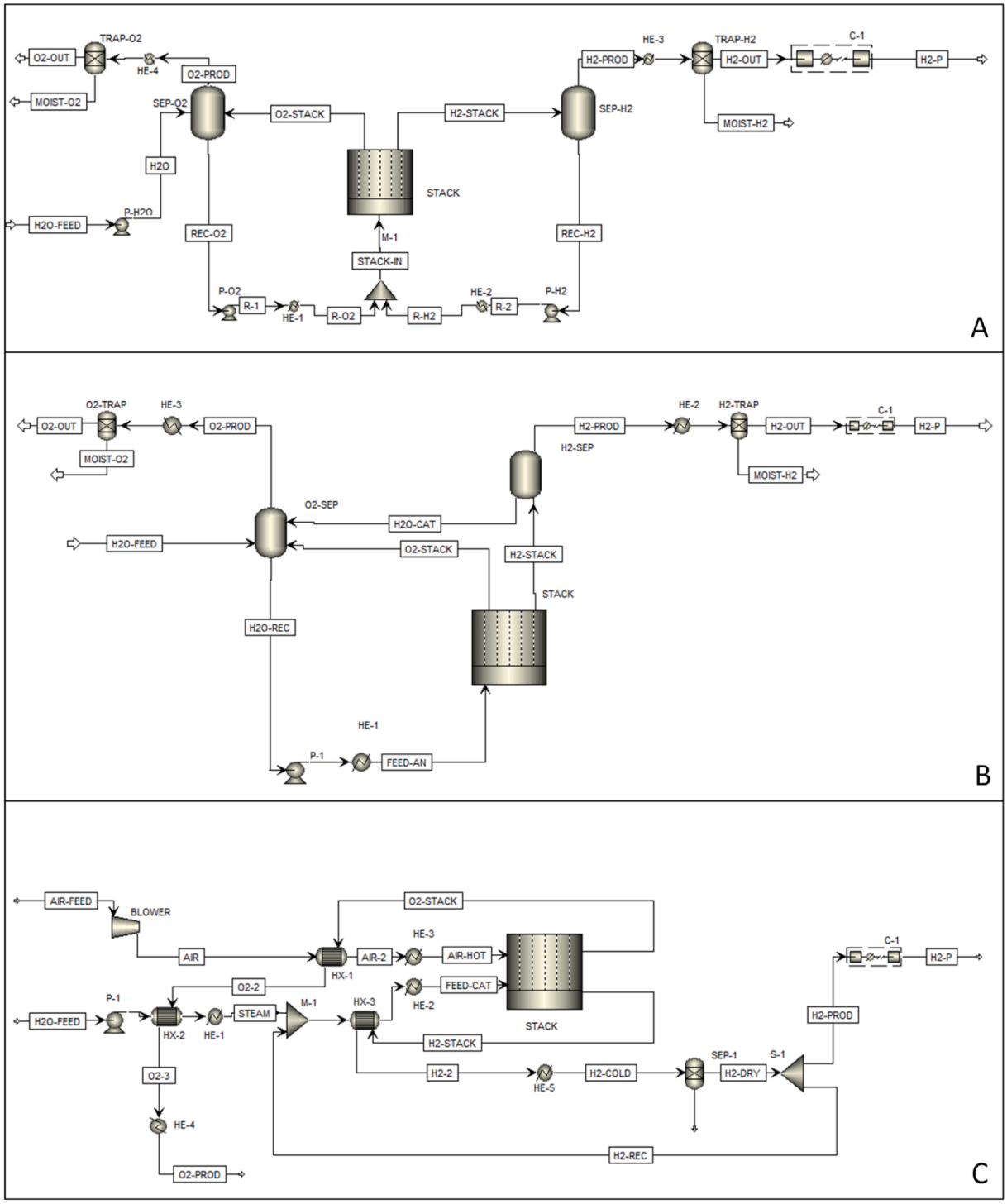


**Fig. 4.** Aspen plus flowsheet of WE processes: AEC (A), PEMEC (B), and SOEC (C). Tags on streams and blocks identify the main streams and unit operations, whose features are summarized in Table S7-S9, respectively.

**Table 1**
Summary of the main characteristics and performances of different electrolysis technologies considered.

| | AEC | PEMEC | SOEC |
|---|---|---|---|
| Electrolyte | KOH (35 wt%) | Nafion® 117 | YSZ |
| Cathode | Ni | Pt | Ni-YSZ |
| Anode | Ni | Ir | LSM-YSZ |
| Cell area ($m^2$) | 4.2 | 0.11 | 0.04 |
| Number of cells | 100 | 500 | 8880 (740x12) |
| Operating temperature (°C) | 80 | 60 | 800 |
| Current density ($A/m^2$) | 2500 | 16,000 | 2500 |
| Stack power (MW) | 1.80 | 1.79 | 1.25 |
| System efficiency (HHV) | 69.0 | 67.8 | 80.1 |
| Specific electric energy consumption ($kWh/kg_{H2}$) | 56.8 | 57.8 | 37.3 |
| Specific heat energy consumption ($kWh/kg_{H2}$) | 0.26 | 0.36 | 8.3 |
| Lifetime (years) | 20 | 20 | 20 |
| Stack duration (years) [28] | 10 | 5 | 4 |
| Capacity factor | 0.97 | 0.97 | 0.97 |
| Electrolyser cost (€/kW) [54] | 989 | 1173 | 1329 |
| Cost of stack replacement (% CAPEX) [28] | 50% | 60% | 60% |

**Table 2**
Grid and green electrical energy mix [55] and EROEI [56,57] fuels used in the calculations.

| Resource | EROEI | Grid energy mix | Green energy mix |
|---|---|---|---|
| Oil | 7 | 3.158% | 0% |
| Natural Gas | 8 | 44.29% | 0% |
| Coal | 17 | 4.579% | 0% |
| Nuclear | 14 | 4.632% | 0% |
| Hydro | 84 | 19.48% | 44.94% |
| PV | 25 | 8.275% | 19.09% |
| Waste | 2 | 1.761% | 4.064% |
| Biofuels | 2 | 5.654% | 13.05% |
| Wind | 18 | 6.247% | 14.41% |
| Geothermal | 9 | 1.926% | 4.443% |
| Tide | 3 | 0.003% | 0.007% |

processes, variable OPEX refer to all necessary consumables excluding fuel costs, such as water, chemicals, and catalysts, whilst fixed OPEX refer to direct labour, administration/general overheads, insurance/local taxes and maintenance. Altogether, annual OPEX are taken as a fixed percentage of CAPEX, namely equal to 8.7% for SMR, and to 9.5% for SMR + CCS [59].

For electrolysis, variable OPEX refer to annuitized stack replacement costs, which are estimated as reported in Table 1, and to the cost of water feed [60]. Fixed OPEX, like for reformers, refer to direct labour, administration/general overheads, insurance/local taxes and maintenance. Electrolyser fixed OPEX costs are most commonly modelled as a fraction of the original CAPEX, independent of the electrolyser type. Most studies put this value between 1 and 3% of the electrolyser CAPEX [61]. Here, a fixed OPEX cost equal to 2% of the total CAPEX is adopted, according to the methodology reported by Glenk et al. [60]. By adding the variable OPEX costs, they amount to 3.06%, 4.6% and 5.45% of CAPEX for AEC, PEMEC and SOEC, respectively.

For all the technologies considered, CAPEX and OPEX estimates include (i) the cost of hydrogen compression equipment to produce hydrogen gas suitable to be used in fuel cell-vehicles (i.e., 300 bar); (ii) the cost of the hydrogen storage tank and (iii) the cost of the hydrogen refuelling dispenser.

### 2.7. Energy Return on Energy Invested

Several methods and indices can be used to assess the efficiency of production processes involving the generation of energy carriers (electricity and/or hydrogen), but the best method for comparing different energy production industries is the Net Energy Analysis (NEA). The goal of NEA is to calculate whether the energy produced by any process considered is greater than the one required to build, operate and maintain the infrastructure. Among the possible indexes derived from NEA, the most suitable indicator for the processes of interest is the EROEI, defined as:

$$EROEI = E_{out}/E_{in} \tag{2}$$

where $E_{out}$ is the available energy that the process provides (GWh). In the case of hydrogen production processes, $E_{out}$ is defined as:

$$E_{out} = (HHV_{H2} \cdot Q_{H2} - P_{aux}) \cdot cf \cdot L \tag{3}$$

where $HHV_{H2}$ is the higher heating value of hydrogen (kWh/kg), $Q_{H2}$ is the flow rate of hydrogen produced (kg/h), $cf$ is the capacity factor (namely the fraction of time the process is productive), $P_{aux}$ is the power consumed by process auxiliaries (kW) and $L$ is the estimated total time of operation of the production process (hours).

$E_{in}$ is defined as:

$$E_{in} = E_{cap} + E_{o\&m} + E_f \tag{4}$$

In equation (4) $E_{in}$ is the total energy provided and consumed during the production and operations periods of the plant, and is made up of three contributions: $E_{cap}$ is the capital energy embodied in the materials and used for construction and decommissioning of the plant; $E_{o\&m}$ is the energy needed for operating and maintaining the plant; $E_f$ is the energy needed for procuring and distributing the fuels, which includes also the energy used for extracting, refining and transporting the fuels from the production well to the plant. All terms are expressed in GWh for consistency: the EROEI is thus dimensionless.

The capital energy embodied in the materials and used for construction and decommissioning of the plant $E_{cap}$ is defined as follows:

$$E_{cap} = CAPEX/\varepsilon_c \tag{5}$$

where $\varepsilon_c$ is the proportionality coefficient between the costs of energy and CAPEX. In this work $\varepsilon_c$ is considered constant and is evaluated from real plant data [62].

The energy needed for operating and maintaining the power plant, $E_{o\&m}$, is defined as:

$$E_{o\&m} = E_{cap} \cdot L \cdot OPEX_{year} \tag{6}$$

Where $OPEX_{year}$ includes fixed and variable OPEX for each production technology considered. It is expressed as % of CAPEX per year.

$$OPEX_{year} = s_{o\&m} \cdot \left(1 + \frac{CSRE}{CAPEX}\right) \tag{7}$$

where $s_{o\&m}$ is the share of the investment costs dedicated to operation and maintenance. CSRE is the cost [€] for the substitution of the electrolyser's stacks, defined as:

$$CSRE = CAPEX \cdot CRE\% \left(\frac{L}{L_{el}}\right) \quad (8)$$

where $L_{el}$ is the period after which the electrolysers stack should be replaced and CRE% is the cost, expressed in % of CAPEX, for its substitution (Table 1). Clearly, CSRE is equal to 0 for grey and blue hydrogen.

The energy needed for procuring and distributing the fuels, $E_f$, is defined as:

$$E_f = \frac{E_{out}}{\eta \cdot EROEI_{fuel}} \quad (9)$$

where $\eta$ is the efficiency of transformation for the process of interest and $EROEI_{fuel}$ refers to the particular technology that is used to transform the source of energy (natural gas or solar irradiation) into usable energy for the process [9]. Literature values of $EROEI_{fuel}$ from different recent sources are reported in Table 2. They consider all the boundaries of various types of EROEI analyses and the energy losses associated with the processing of fuel as it is transformed from "fuel at the wellhead" to consumer-ready fuels. For electrolysers, the calculation of EROEI is done considering the entire process from the source of energy (the solar energy) to the hydrogen produced.

### 2.8. Levelized cost of hydrogen

The levelized cost of hydrogen (LCOH, €/kg) is an indicator specifically derived for hydrogen as an energy carrier. It is calculated according to Fan et al. [24]:

$$LCOH = \frac{CAPEX + \sum_{t=1}^{N} \frac{OPEX_{year}}{(1+r)^t}}{\sum_{t=1}^{N} \frac{HP_t}{(1+r)^t}} \quad (10)$$

where CAPEX [€] is the initial capital investment, $OPEX_{year}$ [€] is the OPEX at year t, $r$ [%] is the discount rate, and $HP_t$ [$kg_{H2}$/hr] the hydrogen production at year t.

By assuming that $OPEX_{year}$ and $HP_t$ are constant over the years, the equation simplifies as:

$$LCOH = \frac{CAPEX + (EC + OPEX_{year}) \sum_{t=1}^{N} \frac{1}{(1+r)^t}}{HP_t \sum_{t=1}^{N} \frac{1}{(1+r)^t}} \quad (11)$$

where EC is the cost of the source of energy per year (€/year). For electrolysers EC is the cost of the electricity from the grid, which is all the energy required for grid hydrogen and only the part of energy not provided by the photovoltaic plant for the green hydrogen. For green electrolysers EC is defined as follows:

$$EC = P_{elec} \cdot EL_{cost} \cdot (cf \cdot 8760 - 1300) \quad (12)$$

where $P_{elec}$ [MW] is the power from the grid supplied to the electrolysers, $EL_{cost}$ [€/MWh] is the cost of the electricity [63], 8760 is the number of hours per year and 1300 is the annual yield of a 1 kWp photovoltaic plant operating at the considered location [64]. For grid electrolysers, EC is defined as in equation (12), without subtracting the 1300 h corresponding to photovoltaics yield.

For the SMR, EC is the cost of natural gas, which is calculated as follows:

$$EC = Q_{NG} \cdot NG_{cost} \cdot (cf \cdot 8760) \quad (13)$$

where $NG_{cost}$ is the cost of natural gas per cubic meter [63] and $Q_{NG}$ is the input volumetric flow rate of natural gas ($Nm^3$/h).

### 2.9. Total Cost of Ownership

Total Cost of Ownership is the cost to buy something plus the cost to operate it over its useful life, considering the total cost that a business will incur to operate an asset, not just the upfront acquisition cost. The TCO metric was computed for $H_2$ vehicles as well as for their diesel counterparts, used as a benchmark, according to:

$$TCO = \frac{CAPEX + \sum_{t=1}^{N} \frac{OPEX_{year}}{(1+r)^t}}{\sum_{t=1}^{N} \frac{output_t}{(1+r)^t}} \quad (14)$$

Where CAPEX [€] include the cost of the vehicles and of the Refueling Dispenser (RD), and $OPEX_{year}$ [€] include the annual Fuel Cost (FC) and the annual maintenance costs (MC). The numerator is divided by the annual output, which is equal to the annual hours of traction ($ht$) for locomotors, and to the annual distance travelled ($km$) for trucks. More details regarding the calculation of TCO for the different vehicles are reported in the Supplementary Material.

### 2.10. Life cycle assessment

Life Cycle Assessment (LCA) is a methodology for estimating the emissions of products during their whole service lifetime, from raw material extraction and refinement, to manufacturing processes, usage, transports and disposal. LCA framework, which is thoroughly described by ISO Standards [65,66], involves the development of four subsequent steps: Goal and scope, i.e., the definition of the characteristics of the study, Life Cycle Inventory (LCI), i.e., the collection of material and energy balances over the entire life cycle of the product system, Life Cycle Impact Assessment (LCIA), i.e., the assessment of the environmental performance over various environmental compartments using several impact categories scores, and interpretation, to draw conclusions on the outcomes of the study. The findings of such investigations are frequently published using well-established impact methodologies, such as ReCiPe, Environmental Footprint (EF) or Tool for Reduction and Assessment of Chemicals and Other Environmental Impacts (TRACI). The environmental performances of the product systems investigated in this paper have been evaluated using Recipe 2016 Midpoint (H) [67], which adopts the following impact categories: Global Warming Potential (GWP), Fine Particulate Matter Formation (PMFP), Stratospheric Ozone Depletion (ODP), Ionizing Radiation (IRP), Photochemical Oxidant Formation including human Health contributions (HOFP) and Ecosystem quality ones (EOFP), Human Toxicity Potential with cancer (HTPc) and non-cancer (HTPnc)-related impacts, Ecotoxicity Potential related to Freshwater (FETP), Marine (METP) and Terrestrial (TETP) perspectives, Freshwater (FEP) and Marine (MEP) Eutrophication Potential, Terrestrial Acidification (TAP), Land use (LOP), Mineral Resource Scarcity (SOP), Fossil Resource Scarcity (FFP), and Water Consumption Potential (WCP).

The environmental burdens of hydrogen production and hydrogen-based logistic activities have been evaluated through LCA. Firstly, the most environmentally friendly hydrogen production pathways had to be identified within each available technology. Then, they were further assessed, along with dedicated vehicles, storage and refuelling facilities, for the evaluation of the logistic activities within the port area for 20 years. Therefore, in this work, two comparative LCA studies have been performed: the first one was devoted to identify the most sustainable technology for hydrogen production (using "the production of 1 kg of hydrogen" as functional unit), while the second one was a Well-to-Wheel (WTW) analysis focused on the replacement of diesel vehicles for port operations for 20 years, using as functional unit "the average port activities for 20 years". Considering a cradle-to-gate perspective, the system boundary of the first assessment includes the extraction, refinement and transportation of raw materials (including energy and fuels), the construction of the facilities and equipment for hydrogen production and the operation of the plants for the production of 1 kg of hydrogen. The second assessment selected the most sustainable routes for hydrogen production and expanded the scope of the study including the fuel storage and refuelling stations and the production of hydrogen-

fueled and diesel-fueled vehicles in order to compare their usage for performing the same activities over a 20-year period.

Primary data on the hydrogen production processes have been evaluated by means of process simulation (see Table 1 and Supplementary Material), while secondary data have been retrieved within ecoinvent v3.8, using the attributional cut-off allocation model. Process simulation allowed to identify the weight of SMR and CCS equipment, the electricity and heat demand, the raw materials consumption and the major process emissions of all the processes. The assessment published by Zhao et al. [68] was used as the source of information for electrolysers' stacks and BoP. For the photovoltaic plant installation, the assumptions adopted by Barbera et al. [15] were used, except that the plant was installed on flat roofs.

Among the alternative hydrogen production processes, the most environmentally friendly from each technology has been compared with a traditional diesel option in a WTW cradle-to-grave comparative LCA study, aiming at identifying the best pathway for carrying out port operations. The average port activities require the simultaneous usage of 5 locomotors (5-year lifetime) for 18 hr/day and 15 trucks (10-year lifetime) running for 300 km/day. Since hydrogen production is not continuous due to the required maintenance of the hydrogen production plant (quantified by the capacity factor, cf), the diesel-fueled vehicles cannot be completely replaced by hydrogen-fueled ones, as they must support the port activities when hydrogen is not available. Therefore, the port activities throughout the year are considered as a combination of activities supported by diesel-fueled vehicles and hydrogen-fueled ones, based on the capacity factors of the various hydrogen production technologies (0.8 for SMR-based, 0.97 for electrolysis-based). The system boundary includes the complete life cycle of the locomotors (diesel or hydrogen-fueled) and trucks (diesel or hydrogen-fueled), the production or procurement of fuels (hydrogen or diesel, respectively), the storage and refuelling equipment and the fuel usage for 20 years. The vehicles characteristics in terms of total lifetime, specific fuel consumption, scheduled activities and maintenance have been specified by the Trieste port authority.

## 3. Results and discussion

Process simulations allowed to obtain rigorous solutions of detailed material and energy balances for the hydrogen production processes of interest, which are necessary for the correct evaluation of the EROEI, LCOH, LCA and TCO indicators. When comparing different production technologies by means of quantitative indicators, it is of critical importance that the data required for their calculation are obtained based on the same assumptions, and with reference to the specific application of interest. Accordingly, the development of process simulations specifically referred to the production capacity considered ensures the consistency of material and energy balances, as well as of equipment size, among the different processes. Process simulations took in consideration all the details of the different processes considered, including thermodynamic and phase equilibria, chemical and electrochemical reactions kinetics, transport phenomena and physical properties. All these quantities have been estimated using reliable models, able to correctly describe the phenomena involved in the processes. The material and energy balances for each unit operation have been solved aiming to quantify the input and output flows for the entire production processes, in order to finally supply the data reported in Table 3, to be used for the calculation of each indicator. A schematic of the connections between source of information (PS, Literature, Assumption/communication), parameters and indicators is shown in Fig. 5.

Table 4 summarizes the values obtained by means of process simulation applied to the SMR process with and without the CCS (grey and blue hydrogen). For blue hydrogen, both the tail gas and the flue gas carbon capture configurations have been considered. Table 4 shows that, for a given hydrogen production, both the total plant cost (CAPEX) and operational costs (OPEX) increase when CCS is added. The increase in CAPEX is higher when CCS is applied to the flue gas stream, due to the larger equipment needed. As a consequence of the increased energy expenditure for carbon capture, the total plant efficiency decreases. On the other hand, the addition of CCS leads to a substantial reduction of the carbon emission factors. However, it should be noted that applying CCS to the tail gas stream only reduces the direct $CO_2$ emissions by 42% compared to those of grey hydrogen, whereas extending it also to the flue gases a 90% decrease can be achieved. Clearly, these numbers are referred just to the direct $CO_2$ emissions of the process, while the actual Global Warming Potential (GWP) is evaluated by LCA and is presented later.

The detailed values obtained by means of process simulation applied to the three electrolysers considered are presented in Table 5. For each electrolyser technology, both green hydrogen and grid hydrogen options have been evaluated. For green hydrogen, the required electrical energy is provided by the installed PV plant when in operation, and by the grid from a fully green energy provider for the remaining time. For grid hydrogen, instead, all the necessary electrical energy is taken from the grid using the Italy energy mix (see Table 2).

Data of CAPEX and OPEX reported in Table 4 and 5 refer to the hydrogen production processes investigated as well as the inclusion in the plant of 12 hydrogen storage tanks of approximately 70.8 kg capacity each at 300 bar. Each hydrogen storage tank is a stainless-steel seamless cylinder of 12.5 m length and 0.61 m diameter, with volume

**Table 3**
Summary of data for the estimation of EROEI, LCOH, TCO and LCA.

| Data | Units | EROEI | LCOH | LCA | TCO |
|---|---|---|---|---|---|
| Hydrogen production ($Q_{H2}$) | kg/h | X | X | X | |
| Higher heating value of hydrogen (HHV) | kWh/kg | X | | X | |
| Power for auxiliary ($P_{aux}$) | % | X | X | X | |
| Input flow rate of natural gas | $Nm^3/h$ | X | X | X | |
| Total plant cost (CAPEX) | € | X | X | | X |
| Ratio between CAPEX and energy cost for construction ($\varepsilon_c$) | €/kWh | X | | | X |
| Capacity factor (cf) | – | X | X | X | X |
| Plant lifetime (L) | years | X | X | X | X |
| Efficiency ($\eta$) | – | X | | | |
| Share of investment costs for operation - maintenance ($s_{o\&m}$) | % | X | X | | X |
| EROEI fuels | – | X | | | |
| Cost of stack replacement (CAPEX %) | % | X | X | | X |
| Stack lifetime | years | X | X | X | X |
| Grid power supply | MW | | X | X | |
| Annual cost of energy (electricity / natural gas) | € | | X | | X |
| Total amount of materials | kg | | | X | |
| Discount rate | % | | X | | X |
| Vehicles purchase cost | € | | | | X |
| Refuelling dispenser cost | € | | | | X |

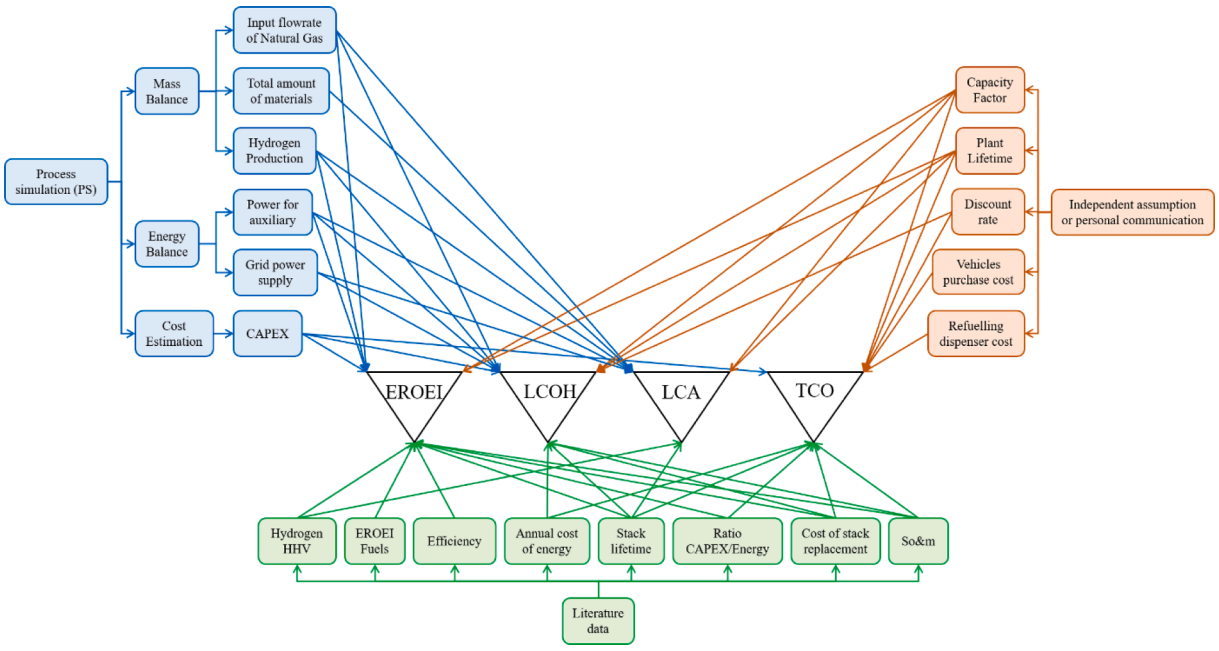


**Fig. 5.** Connections between source of information, parameters and indicators.

**Table 4**
Summary of the numerical data used for the evaluation of the performance indicators for grey and blue hydrogen.

| Data | Units | SMR | CCS tail gas | CCS flue gas |
|---|---|---|---|---|
| Hydrogen production flow rate | kg/h | 32.5 | 32.5 | 32.5 |
| Input flow rate of natural gas | $Nm^3/h$ | 187.5 | 187.5 | 187.5 |
| Higher heating value of hydrogen (HHV) | kWh/kg | 39.4 | 39.4 | 39.4 |
| % of power (kW) for auxiliary | % | 0.1406 | 0.2246 | 0.2587 |
| CAPEX plant including compressors | k€ | 7966.27 | 12127.20 | 13957.23 |
| CAPEX Buffer Tanks and Refuelling Station | k€ | 1060 | 1060 | 1060 |
| CAPEX compressors to 300 bar | k€ | 3474.9 | 3474.9 | 3474.9 |
| Ratio between CAPEX and energy cost for construction ($\varepsilon_c$) | €/kWh | 0.656 | 0.656 | 0.656 |
| capacity factor (cf) | | 0.8 | 0.8 | 0.8 |
| Plant life time (L) | years | 20 | 20 | 20 |
| Efficiency (η) | | 0.760 | 0.690 | 0.690 |
| Share of investment costs for operation - maintenance ($s_{o\&m}$) | % | 0.087 | 0.095 | 0.095 |
| EROEI fuels | | 8 | 8 | 8 |
| Discount rate | % | 0.073 | 0.073 | 0.073 |

of 3.3 $m^3$, thickness of 1.8 cm and weight of 3450 kg. The plant includes also a hydrogen refuelling dispenser with CAPEX estimated to be 60.000 €.

A comparison among the three electrolysers considered for green hydrogen production shows that, for a given hydrogen production, SOEC is the technology that requires less electrical energy thanks to the high operating temperature that favours the kinetics and thermodynamics of the electrolysis process, which is however compensated by a higher need of energy for auxiliaries. Owing to the different technological maturity, the lowest CAPEX is that of AEC and the highest that of SOEC. The maintenance costs are similar among the electrolysers, except for the cost of stacks replacement, which is significantly higher for SOEC, mainly due to lower duration of the stacks with respect to the other two technologies. The lower electrical energy requirement of SOEC reflects in a lower investment for the photovoltaic plant. As far as grid hydrogen is concerned, the main difference is related to the absence of the photovoltaic plant in the system, which lowers the CAPEX compared to green hydrogen, but is balanced by a higher cost of electricity taken form the grid.

The comparison among all the production technologies investigated is better performed by using the indicators described in Section 2. Table 6 summarizes the results obtained in terms of EROEI (equation (2)), LCOH (equation (11), and TCO (equation (14)). As expected, EROEI is relatively low for the SMR process, and is even lower when CCS is added to reduce the $CO_2$ emissions (the value is reduced by 30% and 37% in the tail gas and flue gas capture scenario, respectively). In fact, although the heat duty for the amine solvent regeneration can be satisfied exploiting the heat from the flue gases of the SMR process, a large impact on the overall energy consumption of CCS is related to $CO_2$ compression for subsequent transport and storage. EROEI literature values of grey hydrogen range between 2 and 3 [27], slightly higher than the value reported in Table 6, but this can be justified by the reduced dimension of the plant considered in this paper.

On the other hand, EROEI values for electrolysers are higher compared to the SMR-based processes, and are well in line with literature values [27]. This can be attributed to the higher value of $EROEI_{fuels}$ of the energy mix characterizing green and grid hydrogen, compared to that of natural gas (Tables 4 and 5). Specifically, AEC and PEMEC display higher values with respect to SOEC: this is due to the thermal energy produced by SOEC, which is not included in the calculation of the output energy.

Concerning LCOH, the values reported in Table 6 show that the cost of hydrogen produced by SMR without CCS is comparable with that obtained by electrolysers and, as expected, the cost raises if CCS is applied. This result is somehow in contrast with what reported in the literature, where LCOH of grey and blue hydrogen range between 1.5 and 2.5 €/kg, while for green hydrogen it is between 3 and 9 €/kg [54,69]. The generally higher costs found in this analysis are also due to the contribution of hydrogen compression up to 300 bar. This contribution is often neglected, or taken into account to lower extents (P = 100–200 bar [54]), despite its significant impact on cost evaluation. Nonetheless, this step is necessary if $H_2$ is to be put into the tanks of fuel cell vehicles, as in this case. As also reported in Table 6, the LCOH calculated without accounting for hydrogen compression is in fact in line with literature values for electrolysis processes, while it is still higher for grey and blue hydrogen. This is due to the reduced size of the processes investigated with respect to the ones used for large scale

**Table 5**
Summary of the numerical data used for the evaluation of the performance indicators for green and grid hydrogen.

| Data | Units | AEC | AEC - grid | PEMEC | PEMEC - grid | SOEC | SOEC - grid |
|---|---|---|---|---|---|---|---|
| Hydrogen production flow rate | kg/h | 33.27 | 33.27 | 33.09 | 33.09 | 33.38 | 33.38 |
| Higher heating value of hydrogen (HHV) | kWh/kg | 39.4 | 39.4 | 39.4 | 39.4 | 39.4 | 39.4 |
| % of power (kW) for auxiliary | % | 0.0772 | 0.0772 | 0.1030 | 0.1030 | 0.3005 | 0.3005 |
| Electrical power for electrolysers | MW | 1.891 | 1.891 | 1.912 | 1.912 | 1.365 | 1.365 |
| CAPEX plant including compressors | k€ | 6315.8 | 6315.8 | 7186.9 | 7186.9 | 7588.0 | 7588.0 |
| CAPEX Tanks & Refuelling Station | k€ | 1060 | 1060 | 1060 | 1060 | 1060 | 1060 |
| CAPEX PV plant | k€ | 1701 | 0 | 1720 | 0 | 1229 | 0 |
| CAPEX compressors to 300 bar | k€ | 3474.9 | 3474.9 | 3474.9 | 3474.9 | 3474.9 | 3474.9 |
| Ratio between CAPEX and energy cost for construction ($\varepsilon_c$) | €/kWh | 0.656 | 0.656 | 0.656 | 0.656 | 0.656 | 0.656 |
| capacity factor (cf) | | 0.97 | 0.97 | 0.97 | 0.97 | 0.97 | 0.97 |
| Plant life time (L) | years | 20 | 20 | 20 | 20 | 20 | 20 |
| Stack lifetime | years | 10 | 10 | 5 | 5 | 4 | 4 |
| Cost of stack replacement (CAPEX %) | % | 0.5 | 0.5 | 0.6 | 0.6 | 0.6 | 0.6 |
| Round trip efficiency (η) | | 0.850 | 0.850 | 0.850 | 0.850 | 0.850 | 0.850 |
| Share of investment costs for operation - maintenance(excluding stack substitution), $s_{o\&m}$ | % | 0.020 | 0.020 | 0.020 | 0.020 | 0.020 | 0.020 |
| EROEI fuels | | 46 | 25 | 46 | 25 | 46 | 25 |
| Discount rate | % | 0.073 | 0.073 | 0.073 | 0.073 | 0.073 | 0.073 |

**Table 6**
EROEI and LCOH values for the different hydrogen production technologies, and TCO of fuel cell-vehicles, calculated from data reported in Table 4 and 5. $LCOH_{NC}$ is the LCOH calculated without considering the costs of hydrogen compression to 300 bar.

| Data | Units | SMR | CCS tailgas | CCS fluegas | AEC | AEC - grid | PEMEC | PEMEC - grid | SOEC | SOEC grid |
|---|---|---|---|---|---|---|---|---|---|---|
| $E_{out}$ | GWh | 154.43 | 139.34 | 133.22 | 205.6 | 205.6 | 198.75 | 198.75 | 156.32 | 156.32 |
| $E_{in}$ | GWh | 63.10 | 83.54 | 90.52 | 28.48 | 29.27 | 36.87 | 37.47 | 38.96 | 39.69 |
| EROEI | – | 2.44 | 1.67 | 1.47 | 7.22 | 7.02 | 5.39 | 5.30 | 4.01 | 3.94 |
| LCOH | €/kg | 10.15 | 13.96 | 15.50 | 9.39 | 8.69 | 10.64 | 9.93 | 9.41 | 8.90 |
| $LCOH_{NC}$ | €/kg | 6.50 | 10.15 | 11.69 | 6.29 | 6.32 | 6.79 | 6.86 | 5.58 | 5.65 |
| TCO locomotors | €/hr | 70.25 | 83.10 | 88.28 | 67.69 | 65.32 | 71.92 | 69.52 | 67.76 | 66.05 |
| TCO truck | €/km | 1.73 | 2.16 | 2.34 | 1.65 | 1.57 | 1.79 | 1.71 | 1.65 | 1.59 |

**Table 7**
Numerical data used for the estimation of the TCO.

| Variables | Vehicle | Units | Diesel | Hydrogen |
|---|---|---|---|---|
| Daily hours | Locomotor | h | 18 | 18 |
| Yearly days of operation | Locomotor | h | 365 | 365 |
| Lifetime | Locomotor | years | 5 | 5 |
| Fuel consumption | Locomotor | kg/h | 10.11 | 3.37 |
| Maintenance cost | Locomotor | €/year | 24,500 | 6,125 |
| Purchase Cost | Locomotor | € | 250,000 | 865,000 |
| Daily travel distance | Truck | km | 300 | 300 |
| Yearly days of operation | Truck | days | 365 | 365 |
| Lifetime | Truck | years | 10 | 10 |
| Fuel consumption | Truck | kg/100 km | 33.9 | 11.30 |
| Maintenance cost | Truck | €/year | 9,570 | 7,656 |
| Purchase Cost | Truck | € | 150,000 | 330,000 |
| Refuelling dispenser (€) | Both | € | 10,000 | 60,000 |

production, and can be explained considering the different behaviour of SMR/CCS and electrolysers in the scale-up process: LCOH of electrolysers is in fact rather stable with the equipment size due to the modular nature of these systems, while LCOH of SMR and CCS is strongly affected by the plant size due to economy of scale [59]. Furthermore, the price of natural gas [63] plays a relevant role in the evaluation of the LCOH for these processes, while for electricity-based production processes its effect is mitigated by the contribution of other electricity generation sources.

The TCO data (in € per hour or per km of use of vehicles) are also reported in Table 6, where locomotors and trucks have been analysed separately. The values of TCO include the compression of hydrogen and storage at 300 bar, since the normal refuelling dispenser operates at high pressure. As far as locomotor's TCO is concerned, the reference value of a diesel locomotor is evaluated to be 39.9 €/hr [44]. The TCO data, summarized in Tables 6 and 7, highlight that:

(i) annual fuel expenses of hydrogen-fueled locomotive are similar, sometimes lower, than those of the diesel-fueled locomotive. They are lower when hydrogen is produced with the following production processes (in ascending order): AEC – grid, SOEC – grid, AEC, SOEC, PEMEC – grid.

(ii) the overall OPEX, including annual fuel expenses and maintenance & repair costs, of the hydrogen-fueled locomotive is most often lower than that of diesel-fueled locomotive;

(iii) hydrogen-fueled locomotive have a CAPEX more than three times as high as that of the diesel-fueled locomotive. This depends on the higher acquisition cost of the hydrogen-fueled locomotive, not yet produced at scale;

(iv) as a result, the TCO of the hydrogen-fueled locomotive (ranging from 65.32 €/hour of traction to 88.28 €/ hour of traction) is always higher than that of the diesel-fueled truck (39.39 €/ hour of traction).

As far as truck's TCO is concerned, the reference value for a diesel truck is estimated to be 1.11 €/km. The TCO data for trucks highlight that:

(i) annual fuel expenses of hydrogen-fueled trucks are similar, and sometimes lower, than those of the diesel-fueled truck. They are lower when hydrogen is produced by water electrolysis (either green or grid);

(ii) the overall OPEX, including annual fuel expenses and maintenance & repair costs, of the hydrogen-fueled truck is similar and sometimes lower than that of diesel-fueled truck;

(iii) hydrogen-fueled trucks have a CAPEX more than twice as high as that of the diesel-fueled truck, and this depends on the higher acquisition cost of the hydrogen-fueled truck, not yet produced at scale, and on the higher cost of the refuelling station;

(iv) as a result, the TCO of the hydrogen-fueled truck (ranging from 1.57 €/km to 2.34 €/km) is always higher than that of the diesel-fueled truck (1.11 €/km), irrespectively of the process used to produce hydrogen.

The normalized results of LCA are shown in Fig. 6, highlighting the environmental performance within defined production technologies

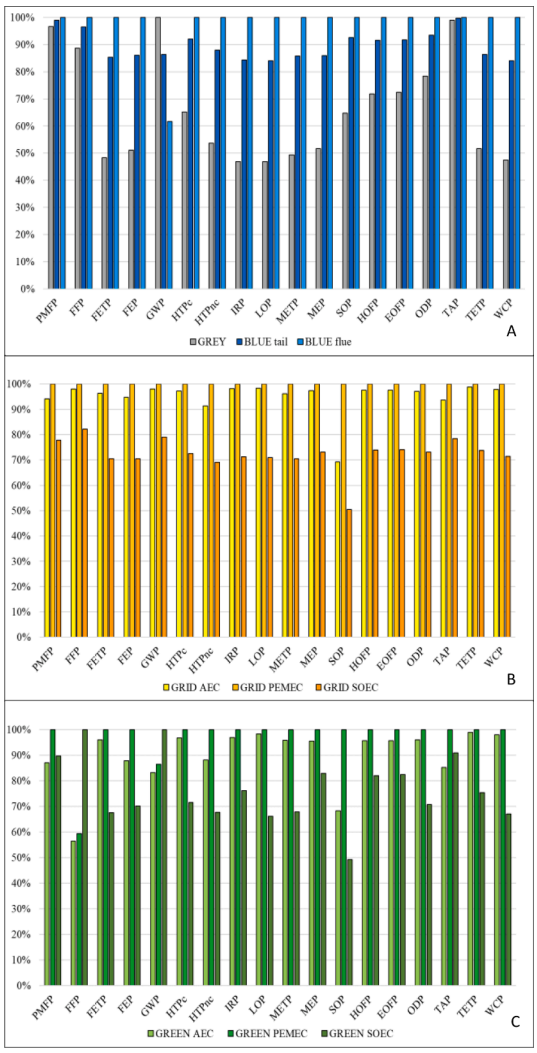


**Fig. 6.** LCIA outcomes normalized for the production of 1 kg of hydrogen for each colour.

groups. The absolute scores of the different impact categories investigated are reported in the Supplementary Material. It is first worthwhile examining the outcomes of different options within a specific hydrogen colour, in order to identify the most sustainable route among similar technologies, which will be further compared with other production pathways.

The analysis of hydrogen produced utilizing SMR, either alone (grey hydrogen), or in combination with CCS (blue-tail and blue-flue) shows that, except for GWP, all the other impact categories are negatively affected by CCS (Fig. 6A). This is due to the carbon capture process, which certainly reduces direct carbon dioxide emissions, but requires increased material and energy expenses, thus worsening blue hydrogen environmental performances overall. Therefore, from a sustainability standpoint, blue hydrogen does not seem so appealing, which makes grey hydrogen worth to be considered for comparison with other promising technologies, even if its $CO_2$ emissions are not mitigated by any capture system. Anyway, it is essential to identify a low-carbon technology to be further compared with hydrogen from water electrolysis. Due to its lower GWP rating compared to the tail gas capture option, blue hydrogen capturing flue gas emissions was chosen for further investigations.

Focusing on electrolysis-based technologies, when the entire energy requirement is supplied through the national grid (grid hydrogen) SOEC technology is undoubtedly the most environmentally friendly, as it shows the lowest impacts among the vast majority of impact categories compared to the other electrolysis technologies (Fig. 6B). This is mainly due to the lower amount of electricity required, which has a significant impact on the performances of electrolysis technologies.

On the other hand, when considering green hydrogen production (Fig. 6C), the selection of the most sustainable technology required a detailed examination of the impact categories. PEMEC is clearly the most burdensome technology, performing poorly in sixteen of the eighteen impact categories, due to the high impacts of the electrolysers, which require large amounts of noble metals, and to the high electricity need. The situation is better for AEC, which usually places in second position and SOEC, which generally gained the best environmental performances, thanks to the lowest electricity consumption. AEC shows worse results in the categories where the effect of renewable electricity production is more significant, such as toxicity potentials (FETP, METP, TETP, HTPc, HTPnc) and SOP due to raw materials extraction. Moreover, the higher AEC scores for ODP, ozone formation (HOFP, EOFP) and IR are related to the electricity production, while for eutrophication (FEP, MEP), land use (LOP) and water use (WCP) are mainly generated by land and biofuels procurement. On the other hand, SOEC technology performs worse in terms of greenhouse gas emissions, due to the need for heat generation using natural gas, resulting in higher scores for GWP and FFP. Since the development of alternative hydrogen synthesis pathways is primarily focused on reducing GHG emissions, AEC has been selected as the most sustainable green hydrogen technology, thanks to its better GWP outcomes, SOEC's low technology readiness level (TRL), and AEC's overall general performance, also in terms of EROEI and LCOH.

After the selection of the less burdensome hydrogen production processes among the different technologies, these have been considered within the WTW analysis, along with the traditional diesel-based option, as shown in Fig. 7.

Activities supported by green hydrogen gained the lowest impacts for 6 out of 18 impact categories, generally related to burdens generated by combustion processes, while diesel-based activities generate lowest emissions for 10 out of 18 impact categories, mainly thanks to the usage of a reduced amount of electricity though the lifecycle. Activities supported by SMR-based hydrogen (with or without CCS) are generally more burdensome than diesel-based ones (except for HOFP, EOFP, ODP and TETP), indicating that the replacement of diesel vehicles is not convenient from an environmental standpoint, if hydrogen is produced using fossil fuels such as natural gas. An even worst behaviour is shown by grid hydrogen, which is the most burdensome for 8 impact categories, whose results are mainly influenced by the high electricity usage coming from the grid. In terms of GWP, the port activities supported by green hydrogen are the ones that generate the lowest amount of greenhouse gases, with a score about half of that of blue hydrogen, which is the second-best option, followed by diesel, grey hydrogen and grid hydrogen ones. Note that activities supported by grid hydrogen, despite being based on a carbon-free feedstock, performs very poorly in terms of emissions because of the high specific energy consumption, which is derived by more than 50% from fossil sources. As a result, the use of alkaline electrolysers supplied with renewable energy produced by a dedicated photovoltaic plant complemented by a green energy mix is the best option to reduce GHG emissions and, in general, most of the indicators related to air pollution. However, care must be taken to minimize environmental impacts when different natural compartments are considered, particularly dealing with the impact categories where green hydrogen shows the worst performances. They are primarily related to the use of electricity, which accounts for 65 to 99 % of each individual impact (FETP, LOP, METP, WCP), or raw materials extraction and consumption, which accounts for about 54% of HTPc, HTPnc and SOP. The electricity emissions are mostly related to the construction and maintenance of the electricity grid, and the production of electricity using biofuels and other material-intensive technologies. Indeed, the extraction and processing of raw materials (especially metals) releases

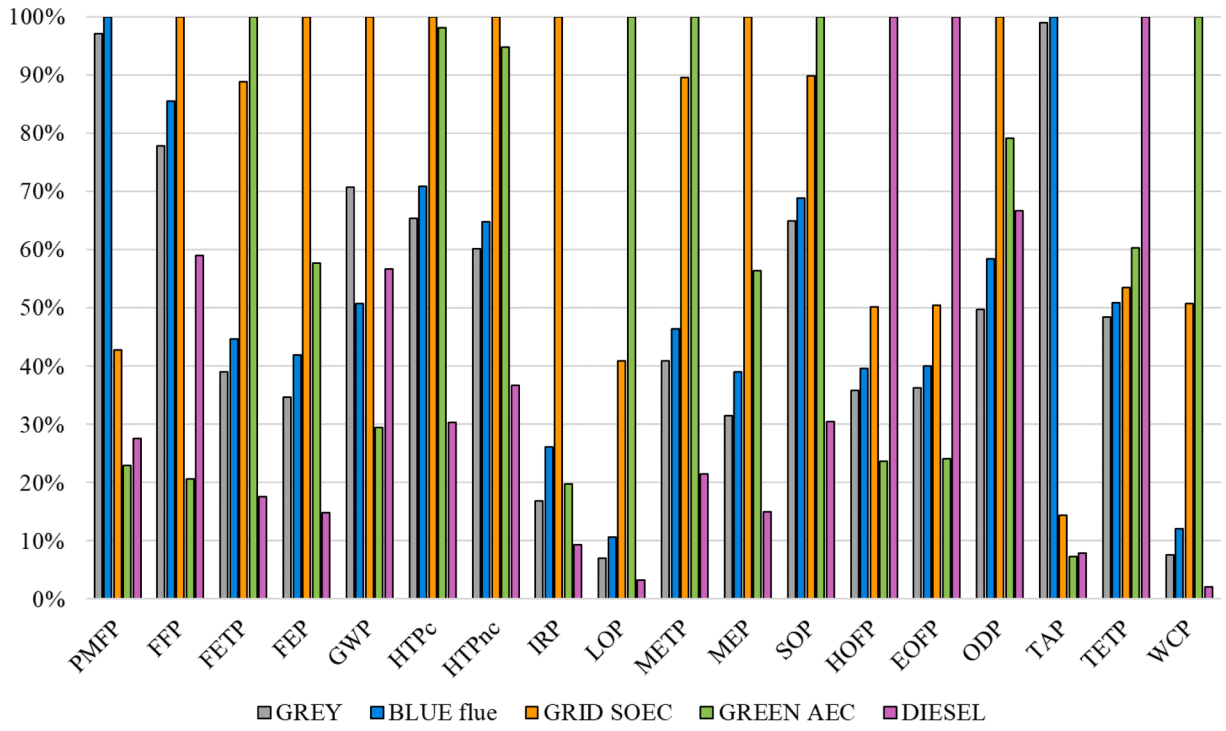


**Fig. 7.** Normalized LCIA outcomes for the comparative WTW analysis, considering the whole port logistic activities for 20 years.

hazardous compounds into the air and the aquatic environment, whereas the use of biofuels derived from dedicated plantations increases the need of fertilizers and land usage. This is aligned with other studies published in the scientific literature [70]. Therefore, it would be necessary to adopt less burdensome strategies for generating renewable electricity, such as minimizing the impact of the mining industry and avoiding the need of plantations dedicated to the production of biofuels. In this regard, there is a wide margin for improvement. Concerning land usage (LOP) green hydrogen appears to have a significantly larger impact compared to any other alternative, however the absolute score is equal to less than 1 $m^2/kgH_2$ (Supplementary Material), which does not pose a concern.

## 4. Conclusions

The aim of this work was to set up a novel procedure for the assessment of the sustainability of production and use of hydrogen as a locally produced alternative fuel to drive shunting locomotors and yard trucks in port logistic operations. A major contribution of the paper is the extension of process simulation methodology to tackle a novel multidisciplinary approach allowing a rigorous estimate of indicators such as the Energy Return on Energy Invested (EROEI), the Levelized Cost of Hydrogen (LCOH), the Life Cycle Assessment (LCA) and the Total Cost of Ownership (TCO). This methodology is entirely based on systematic process simulations, and therefore can be done at the design time during the development of a new process, without requiring real plant operation data.

A number of hydrogen production processes were modelled, including steam methane reforming with and without carbon capture and storage (grey and blue hydrogen), and water electrolysis based on different electrolyzers technologies and powered by fully renewable sources (green hydrogen) or by the national energy grid (grid hydrogen).

As a case study, the Port of Trieste was investigated, since it can be a benchmark for medium-sized Mediterranean port in rapid expansion and with the port authority strongly interested in investing to develop a hydrogen-based logistics. However, the proposed methodology is general and can be applied to any port or to any logistic centre in which trucks, trains and other means of transportation are present. It can be a powerful tool for policy decision-makers in defining the strategies for the development of hydrogen-based transport systems in ports.

Through a comparison of the different indicators' values for the production processes under investigation, it was concluded that green hydrogen is a valuable option from a sustainability viewpoint. Indeed, it shows excellent energetic performance, addressed by EROEI, while data on LCOH show that, when hydrogen is produced at local level, green hydrogen results to be also economically convenient if compared to blue hydrogen. Regarding the TCO, the value of hydrogen-fueled locomotors and trucks is presently larger than the one for diesel-fueled ones, but this result depends the huge difference in the purchase price of the former, which is expected to fall sharply once hydrogen-based port operations will be enforced in the next future.

The environmental burdens of hydrogen production and hydrogen-based logistic activities showed that, when compared to diesel-based traditional logistic activities, a consistent reduction of GHG emissions is ensured only by green hydrogen. However, a larger perspective reveals that there is still room for improvement regarding other environmental categories, where the impacts of activities supported by green hydrogen are larger than the ones based on other hydrogen synthesis pathways or diesel ones. They are mainly related to emissions from electricity generation and the extraction of raw materials, for which less burdensome practices must be devised. Due to its large electricity consumption, grid hydrogen showed worse overall performances with respect to green hydrogen, and for numerous impact categories even with respect to grey one or diesel. Grey and blue hydrogen-fueled operations resulted more impactful than diesel-fueled ones in most impact categories, depending on the specific emissions associated with the use of natural gas or diesel. Due to their high $CO_2$ emissions, they are unlikely to be used in the long run.

*CRediT authorship contribution statement*

**Andrea Mio:** Data curation, Formal analysis, Investigation,

Software, Writing – original draft. **Elena Barbera:** Data curation, Formal analysis, Investigation, Software, Writing – original draft. **Alessandro Massi Pavan:** Conceptualization, Writing – review & editing. **Romeo Danielis:** Formal analysis, Investigation, Methodology, Writing – original draft. **Alberto Bertucco:** Conceptualization, Supervision, Writing – review & editing. **Maurizio Fermeglia:** Conceptualization, Data curation, Methodology, Supervision, Writing – original draft, Writing – review & editing.

## Declaration of Competing Interest

The authors declare that they have no known competing financial interests or personal relationships that could have appeared to influence the work reported in this paper.

## Data availability

Data will be made available on request.

## Acknowledgements

This research did not receive any specific grants from funding agencies in the public, commercial, or not-for-profit sectors.

## References

[1] Syvitski J, Waters CN, Day J, Milliman JD, Summerhayes C, Steffen W, et al. Extraordinary human energy consumption and resultant geological impacts beginning around 1950 CE initiated the proposed Anthropocene Epoch. Commun Earth Environ 2020;1:1–13. https://doi.org/10.1038/s43247-020-00029-y.
[2] IPCC. AR6 Synthesis Report: Climate Change 2022 n.d. https://www.ipcc.ch/report/sixth-assessment-report-cycle/ (accessed March 20, 2022).
[3] IEA. Net Zero by 2050 n.d. https://www.iea.org/reports/net-zero-by-2050 (accessed March 20, 2022).
[4] Staffell I, Scamman D, Velazquez Abad A, Balcombe P, Dodds PE, Ekins P, et al. The role of hydrogen and fuel cells in the global energy system. Energy Environ Sci 2019;12:463–91. https://doi.org/10.1039/c8ee01157e.
[5] Fuel Cells and Hydrogen Joint Undertaking. Hydrogen Roadmap Europe. 2019 n.d. https://www.fch.europa.eu/sites/default/files/Hydrogen Roadmap Europe_Report.pdf (accessed March 20, 2022).
[6] MISE. Piano Nazionale di Ripresa e Resilienza 2022. https://www.mise.gov.it/index.php/it/68-incentivi/2042324-piano-nazionale-di-ripresa-e-resilienza-i-progetti-del-mise (accessed March 20, 2022).
[7] Howarth RW, Jacobson MZ. How green is blue hydrogen? Energy Sci Eng 2021;9:1676–87. https://doi.org/10.1002/ese3.956.
[8] Armaroli N, Barbieri A. The hydrogen dilemma in Italy's energy transition. Nature Italy 2021 2021.. https://doi.org/10.1038/d43978-021-00109-3.
[9] Hall CAS, Lambert JG, Balogh SB. EROI of different fuels and the implications for society. Energy Policy 2014;64:141–52. https://doi.org/10.1016/J.ENPOL.2013.05.049.
[10] Eia. Levelized Cost of New Generation Resources in the Annual Energy Outlook 2013. US Energy Information Administration 2022:1–5.
[11] Minutillo M, Perna A, Forcina A, Di Micco S, Jannelli E. Analyzing the levelized cost of hydrogen in refueling stations with on-site hydrogen production via water electrolysis in the Italian scenario. Int J Hydrogen Energy 2021;46:13667–77. https://doi.org/10.1016/J.IJHYDENE.2020.11.110.
[12] EC-JRC. ILCD Handbook — General guide for Life Cycle Assessment. 2010. https://doi.org/10.2788/38479.
[13] Mio A, Bertagna S, Cozzarini L, Laurini E, Bucci V, Marinò A, et al. Multiscale modelling techniques in life cycle assessment: Application to nanostructured polymer systems in the maritime industry. Sustain Mater Technol 2021;29:e00327.
[14] Petrescu L, Burca S, Fermeglia M, Mio A, Cormos CC. Process simulation coupled with LCA for the evaluation of liquid - liquid extraction processes of phenol from aqueous streams. J Water Process Eng 2021;41:102077. https://doi.org/10.1016/J.JWPE.2021.102077.
[15] Barbera E, Mio A, Massi Pavan A, Bertucco A, Fermeglia M. Fuelling power plants by natural gas: An analysis of energy efficiency, economical aspects and environmental footprint based on detailed process simulation of the whole carbon capture and storage system. Energy Convers Manag 2022;252:115072. https://doi.org/10.1016/J.ENCONMAN.2021.115072.
[16] Cigolotti V. The role of hydrogen in European port ecosystems. Energia, Ambiente e Innovazione 2021;1:139–43. https://doi.org/10.12910/EAI2021-027.
[17] Cullen DA, Neyerlin KC, Ahluwalia RK, Mukundan R, More KL, Borup RL, et al. New roads and challenges for fuel cells in heavy-duty transportation. Nature Energy 2021 6:5 2021;6:462–74. https://doi.org/10.1038/s41560-021-00775-z.
[18] Gray N, McDonagh S, O'Shea R, Smyth B, Murphy JD. Decarbonising ships, planes and trucks: An analysis of suitable low-carbon fuels for the maritime, aviation and haulage sectors. Advances in Applied Energy 2021;1:100008. https://doi.org/10.1016/J.ADAPEN.2021.100008.
[19] IRENA. How to decarbonise the shipping industry by 2050. 2021.
[20] Ministero dello Sviluppo Economico. Strategia Energetica Nazionale (SEN). 2017.
[21] Ji M, Wang J. Review and comparison of various hydrogen production methods based on costs and life cycle impact assessment indicators. Int J Hydrogen Energy 2021;46:38612–35. https://doi.org/10.1016/j.ijhydene.2021.09.142.
[22] Lee S, Kim HS, Park J, Kang BM, Cho CH, Lim H, et al. Scenario-based techno-economic analysis of steam methane reforming process for hydrogen production. Applied Sciences (Switzerland) 2021:11. https://doi.org/10.3390/app11136021.
[23] Ali Khan MH, Daiyan R, Neal P, Haque N, MacGill I, Amal R. A framework for assessing economics of blue hydrogen production from steam methane reforming using carbon capture storage & utilisation. Int J Hydrogen Energy 2021;46:22685–706. https://doi.org/10.1016/j.ijhydene.2021.04.104.
[24] Fan JL, Yu P, Li K, Xu M, Zhang X. A levelized cost of hydrogen (LCOH) comparison of coal-to-hydrogen with CCS and water electrolysis powered by renewable energy in China. Energy 2022;242:123003. https://doi.org/10.1016/j.energy.2021.123003.
[25] Bauer C, Treyer K, Antonini C, Bergerson J, Gazzani M, Gencer E, et al. On the climate impacts of blue hydrogen production. Sustain Energy Fuels 2022;6:66–75. https://doi.org/10.1039/d1se01508g.
[26] Romano MC, Brandon NP, Bertsch V, Crema L, Brouwer J, Dodds PE, et al. Comment on "How green is blue hydrogen?". Energy Sci Eng 2022. https://doi.org/10.1002/ese3.1126.
[27] Palmer G, Roberts A, Hoadley A, Dargaville R, Honnery D. Life-cycle greenhouse gas emissions and net energy assessment of large-scale hydrogen production via electrolysis and solar PV. Energy Environ Sci 2021;14:5113–31. https://doi.org/10.1039/d1ee01288f.
[28] Zhao G, Kraglund MR, Frandsen HL, Wulff AC, Jensen SH, Chen M, et al. Life cycle assessment of H2O electrolysis technologies. Int J Hydrogen Energy 2020;45:23765–81. https://doi.org/10.1016/j.ijhydene.2020.05.282.
[29] Akhtar MS, Dickson R, Niaz H, Hwang DW, Jay LJ. Comparative sustainability assessment of a hydrogen supply network for hydrogen refueling stations in Korea – a techno-economic and lifecycle assessment perspective. Green Chem 2021;23:9625–39. https://doi.org/10.1039/D1GC03006J.
[30] Li L, Feng L, Manier H, Manier MA. Life cycle optimization for hydrogen supply chain network design. Int J Hydrogen Energy 2022. https://doi.org/10.1016/J.IJHYDENE.2022.03.219.
[31] LCTI: Zero Emissions for California Ports (ZECAP) | California Air Resources Board n.d. https://ww2.arb.ca.gov/lcti-zero-emissions-california-ports-zecap (accessed February 9, 2023).
[32] Barbera E, Mantoan F, Bertucco A, Bezzo F. Hydrogenation to convert CO2 to C1 chemicals: Technical comparison of different alternatives by process simulation. Can J Chem Eng 2020. https://doi.org/10.1002/cjce.23755.
[33] Barbera E, Sforza E, Musolino V, Kumar S, Bertucco A. Nutrient recycling in large-scale microalgal production: Mass and energy analysis of two recovery strategies by process simulation. Chem Eng Res Des 2018;132:785–94. https://doi.org/10.1016/J.CHERD.2018.02.028.
[34] Turton R, Bailie RC, Whiting WB, Shaeiwitz JA. Analysis, Design and Synthesis of Chemical Processes. 2008.
[35] Morais S, Mata TM, Martins AA, Pinto GA, Costa CAV. Simulation and life cycle assessment of process design alternatives for biodiesel production from waste vegetable oils. J Clean Prod 2010;18:1251–9. https://doi.org/10.1016/j.jclepro.2010.04.014.
[36] Azam MU, Vete A, Afzal W. Process Simulation and Life Cycle Assessment of Waste Plastics: A Comparison of Pyrolysis and Hydrocracking. Molecules 2022:27. https://doi.org/10.3390/molecules27228084.
[37] Barbera E, Naurzaliyev R, Asiedu A, Bertucco A, Resurreccion EP, Kumar S. Techno-economic analysis and life-cycle assessment of jet fuels production from waste cooking oil via in situ catalytic transfer hydrogenation. Renew Energy 2020;160:428–49. https://doi.org/10.1016/j.renene.2020.06.077.
[38] Mio A, Petrescu L, Luca AV, Galusnyak SC, Fermeglia M, Cormos CC. Carbon Dioxide Capture in the Iron and Steel Industry: Thermodynamic Analysis, Process Simulation, and Life Cycle Assessment. Chem Biochem Eng Q 2022;36:255–71. https://doi.org/10.15255/CABEQ.2022.2123.
[39] Morales-Mendoza LF, Azzaro-Pantel C, Belaud JP, Ouattara A. Coupling life cycle assessment with process simulation for ecodesign of chemical processes. Environ Prog Sustain Energy 2018;37:777–96. https://doi.org/10.1002/ep.12723.
[40] Kuo PC, Illathukandy B, Kung CH, Chang JS, Wu W. Process simulation development of a clean waste-to-energy conversion power plant: Thermodynamic and environmental assessment. J Clean Prod 2021:315. https://doi.org/10.1016/j.jclepro.2021.128156.
[41] Fan S, Wang X, Lang X, Wang Y. Energy efficiency simulation of the process of gas hydrate exploitation from flue gas in an electric power plant. Nat Gas Ind B 2017;4:470–6. https://doi.org/10.1016/j.ngib.2017.09.009.
[42] Stradioto DA, Seelig MF, Schneider PS. Performance analysis of a CCGT power plant integrated to a LNG regasification process. J Nat Gas Sci Eng 2015;23:112–7. https://doi.org/10.1016/j.jngse.2015.01.032.
[43] Tabat ME, Omoarukhe FO, Güleç F, Adeniyi DE, Mukherjee A, Okoye PU, et al. Process design, exergy, and economic assessment of a conceptual mobile

autothermal methane pyrolysis unit for onsite hydrogen production. Energy Convers Manag 2023:278. https://doi.org/10.1016/j.enconman.2023.116707.
[44] Adriafer. Personal communication n.d.
[45] Aspen Technology Inc. Aspen Plus Ammonia Model 2008.
[46] National Renewable Energy Laboratory (NREL). Equipment Design and Cost Estimation for Small Modular Biomass Systems, Synthesis Gas Cleanup, and Oxygen Separation Equipment; Task 1: Cost Estimates of Small Modular Systems. 2006.
[47] Meerman JC, Hamborg ES, van Keulen T, Ramírez A, Turkenburg WC, Faaij APC. Techno-economic assessment of CO2 capture at steam methane reforming facilities using commercially available technology. Int J Greenhouse Gas Control 2012;9:160–71. https://doi.org/10.1016/j.ijggc.2012.02.018.
[48] Sánchez M, Amores E, Abad D, Rodríguez L, Clemente-Jul C. Aspen Plus model of an alkaline electrolysis system for hydrogen production. Int J Hydrogen Energy 2020;45:3916–29. https://doi.org/10.1016/j.ijhydene.2019.12.027.
[49] Dale NV, Mann MD, Salehfar H. Semiempirical model based on thermodynamic principles for determining 6 kW proton exchange membrane electrolyzer stack characteristics. J Power Sources 2008;185:1348–53. https://doi.org/10.1016/j.jpowsour.2008.08.054.
[50] García-Valverde R, Espinosa N, Urbina A. Simple PEM water electrolyser model and experimental validation. Int J Hydrogen Energy 2012;37:1927–38. https://doi.org/10.1016/j.ijhydene.2011.09.027.
[51] Rivera-Tinoco R, Farran M, Bouallou C, Auprêtre F, Valentin S, Millet P, et al. Investigation of power-to-methanol processes coupling electrolytic hydrogen production and catalytic CO2 reduction. Int J Hydrogen Energy 2016;41:4546–59. https://doi.org/10.1016/j.ijhydene.2016.01.059.
[52] Im-orb K, Visitdumrongkul N, Saebea D, Patcharavorachot Y, Arpornwichanop A. Flowsheet-based model and exergy analysis of solid oxide electrolysis cells for clean hydrogen production. J Clean Prod 2018;170:1–13. https://doi.org/10.1016/j.jclepro.2017.09.127.
[53] Abad D, Vega F, Navarrete B, Delgado A, Nieto E. Modeling and simulation of an integrated power-to-methanol approach via high temperature electrolysis and partial oxy-combustion technology. Int J Hydrogen Energy 2021;46:34128–47. https://doi.org/10.1016/j.ijhydene.2021.04.029.
[54] Christensen A. Assessment of Hydrogen Production Costs from Electrolysis: United States and Europe. 2020.
[55] IEA. Key energy statistics, 2020, Italy n.d. https://www.iea.org/countries/italy.
[56] King LC, Van Den Bergh JCJM. Implications of net energy-return-on-investment for a low-carbon energy transition. Nat Energy 2018;3:334–40. https://doi.org/10.1038/s41560-018-0116-1.
[57] Capellán-Pérez I, de Castro C, Miguel González LJ. Dynamic Energy Return on Energy Investment (EROI) and material requirements in scenarios of global transition to renewable energies. Energ Strat Rev 2019;26:100399. https://doi.org/10.1016/J.ESR.2019.100399.
[58] Douglas JM. Conceptual Design Of Chemical Processes. Singapore: McGraw-Hill Book Company; 1988.
[59] Hydrogen production costs 2021. 2021..
[60] Glenk G, Reichelstein S. Economics of converting renewable power to hydrogen. Nat Energy n.d. https://doi.org/10.1038/s41560-019-0326-1.
[61] Brynolf S, Taljegard M, Grahn M, Hansson J. Electrofuels for the transport sector: A review of production costs. Renew Sustain Energy Rev 2018;81:1887–905. https://doi.org/10.1016/J.RSER.2017.05.288.
[62] Sgouridis S, Carbajales-Dale M, Csala D, Chiesa M, Bardi U. Comparative net energy analysis of renewable electricity and carbon capture and storage. Nat Energy 2019;4:456–65. https://doi.org/10.1038/s41560-019-0365-7.
[63] Italian Regulatory Authority for Energy Networks and Environment (ARERA). Dati e statistiche n.d. https://www.arera.it/it/dati/elenco_dati.htm.
[64] European Commission. Photovoltaic geographical information system n.d. https://re.jrc.ec.europa.eu/pvg_tools/en/.
[65] The International Standards Organisation. ISO 14040 Environmental management — Life cycle assessment — assessment — Principles and framework. vol. 2006. 2006.
[66] The International Standards Organisation. ISO 14044 Environmental management — Life cycle assessment — Requirements and guidelines. vol. 2006. 2006.
[67] Huijbregts MAJ, Steinmann ZJN, Elshout PMF, Stam G, Verones F, Vieira M, et al. ReCiPe2016: a harmonised life cycle impact assessment method at midpoint and endpoint level. Int J Life Cycle Assess 2017;22:138–47. https://doi.org/10.1007/S11367-016-1246-Y/TABLES/2.
[68] Zhao G, Ravn Nielsen E. Environmental Impact Study of BIG HIT. 2018.
[69] International Energy Agency I. Global Hydrogen Review 2021 n.d.
[70] Mehmeti A, Angelis-Dimakis A, Arampatzis G, McPhail SJ, Ulgiati S. Life Cycle Assessment and Water Footprint of Hydrogen Production Methods: From Conventional to Emerging Technologies. Environments 2018, Vol 5, Page 24 2018;5:24. https://doi.org/10.3390/ENVIRONMENTS5020024.